N72-17922

NASA TECHNICAL MEMORANDUM

NASA TM X-2513

NASA TM X-2513

CASE FILE COPY

EFFECT OF CONFIGURATION MODIFICATIONS ON THE LOW-SUBSONIC AERODYNAMIC CHARACTERISTICS OF A SPACE SHUTTLE-ORBITER CONCEPT WITH A BLENDED DELTA WING-BODY

by Delma C. Freeman, Jr.

Langley Research Center
Hampton, Va. 23365

NATIONAL AERONAUTICS AND SPACE ADMINISTRATION • WASHINGTON, D. C. • FEBRUARY 1972

1. Report No. NASA TM X-2513	2. Government Accession No.	3. Recipient's Catalog No.
4. Title and Subtitle EFFECT OF CONFIGURATION MODIFICATIONS ON THE LOW-SUBSONIC AERODYNAMIC CHARACTERISTICS OF A SPACE SHUTTLE-ORBITER CONCEPT WITH A BLENDED DELTA WING-BODY		5. Report Date February 1972
		6. Performing Organization Code
7. Author(s) Delma C. Freeman, Jr.		8. Performing Organization Report No. L-8093
9. Performing Organization Name and Address NASA Langley Research Center Hampton, Va. 23365		10. Work Unit No. 117-07-01-01
		11. Contract or Grant No.
12. Sponsoring Agency Name and Address National Aeronautics and Space Administration Washington, D.C. 20546		13. Type of Report and Period Covered Technical Memorandum
		14. Sponsoring Agency Code
15. Supplementary Notes		

16. Abstract

An investigation of several configuration modifications to improve the subsonic stability and performance of a blended delta wing-body space shuttle-orbiter concept has been conducted in the Langley low-turbulence pressure tunnel. These modifications included variations in vertical-tail location and orientation, wing planform shape, and afterbody shape. The model was tested at a Reynolds number, based on body length, of 17×10^6, at a Mach number of 0.25, and at angles of attack from about -4^o to 22^o.

17. Key Words (Suggested by Author(s)) Space shuttle vehicles Blended delta wing-body	18. Distribution Statement Unclassified – Unlimited

19. Security Classif. (of this report)	20. Security Classif. (of this page)	21. No. of Pages	22. Price*
Unclassified	Unclassified	61	$3.00

*For sale by the National Technical Information Service, Springfield, Virginia 22151

EFFECT OF CONFIGURATION MODIFICATIONS ON THE LOW-SUBSONIC AERODYNAMIC CHARACTERISTICS OF A SPACE SHUTTLE-ORBITER CONCEPT WITH A BLENDED DELTA WING-BODY

By Delma C. Freeman, Jr.
Langley Research Center

SUMMARY

An investigation of several configuration modifications to improve the subsonic stability and performance of a blended delta wing-body space shuttle-orbiter concept has been conducted in the Langley low-turbulence pressure tunnel. These modifications included variations in vertical-tail location and orientation, wing planform shape, and afterbody shape. The model was tested at a Reynolds number, based on body length, of 17×10^6, at a Mach number of 0.25, and at angles of attack from about -4° to 22°.

The results of the investigation indicate that removing the tip fins and adding a center-line vertical tail increased the maximum trimmed lift-drag ratio from 3.4 to 5.1 and that extending the wing trailing edge on the model with the center-tail configuration further increased the trimmed lift-drag ratio to 5.3. Removing the boattailing from the afterbody decreased the trimmed lift-drag ratio by about 0.6. Deflecting the elevons to -30° on the model with the tip-fin configuration increased the directional stability significantly at the high angles of attack and thus caused the model to be stable throughout the test angle-of-attack range. Replacing the tip fins with a center-line vertical tail resulted in no significant changes in the lateral-directional characteristics of the configuration.

INTRODUCTION

One of the current goals of the National Aeronautics and Space Administration is the development of an economical space transportation system capable of placing large payloads in near-earth orbit. As part of this general effort, wind-tunnel tests of a model of a high-cross-range orbiter concept with a blended delta wing-body have been made at the Langley Research Center. Initial investigations of this concept (refs. 1 and 2) indicated unacceptably low aerodynamic performance levels due primarily to excessive trim drag. The present investigation was conducted in the Langley low-turbulence pressure tunnel in an effort to improve the subsonic characteristics of the configuration by modifications to eliminate the large negative pitching moment at zero lift $\left(C_{m,o}\right)$ and therefore reduce the trim-drag penalty. The results presented in reference 1 indicate that much of the large negative $C_{m,o}$ is associated with an interaction of the tip fins and the wing vortex. Therefore, most of the present investigation was devoted to testing of fin modifications. Other modifications such as extended wing trailing edge and altered afterbody were also investigated. The model was tested at a Reynolds number, based on body length, of approximately 17×10^6, at a Mach number of 0.25, at angles of attack from approximately -4^o to 22^o, and at angles of sideslip of 0^o and -6^o.

SYMBOLS

The longitudinal data are referred to the stability system of axes and the lateral-directional data are referred to the body system of axes. (See fig. 1.) The moment center was located at 66.7 percent of the body length, as indicated in figure 2(a).

The units used for the physical quantities of this paper are given both in the International System of Units (SI) and in the U.S. Customary Units. Measurements and calculations were made in U.S. Customary Units.

b — reference wing span, 35.66 cm (14.04 in.)

C_D — drag coefficient, $\frac{\text{Drag}}{qS}$

C_L — lift coefficient, $\frac{\text{Lift}}{qS}$

C_l — rolling-moment coefficient, $\frac{M_X}{qSb}$

$C_{l_\beta} = \frac{\partial C_l}{\partial \beta}$

C_m — pitching-moment coefficient, $\frac{M_Y}{qSl}$

$C_{m,o}$ — pitching-moment coefficient at $C_L = 0$

C_n — yawing-moment coefficient, $\frac{M_Z}{qSb}$

$C_{n_\beta} = \frac{\partial C_n}{\partial \beta}$

$C_{p,c}$ — balance cavity pressure coefficient

C_Y side-force coefficient, $\frac{\text{Side force}}{qS}$

$C_{Y_\beta} = \frac{\partial C_Y}{\partial \beta}$

D drag force, newtons (lb)

F_Y side force, newtons (lb)

L lift force, newtons (lb)

l body length, 66.26 cm (26.087 in.)

M_X rolling moment, m-N (ft-lb)

M_Y pitching moment, m-N (ft-lb)

M_Z yawing moment, m-N (ft-lb)

q dynamic pressure, N/m^2 (lb/ft^2)

S total planform area, 0.121 m^2 (1.302 ft^2)

X,Y,Z body reference axes

x,y coordinates along X-axis and Y-axis, respectively, cm (in.)

α angle of attack, deg

β angle of sideslip, deg

δ_e elevon deflections, positive when trailing edge is down, deg

ψ angle of yaw, deg

Subscript:

s stability axes

DESCRIPTION OF MODEL

The configuration tested was an approximately 0.013-scale model of a high-cross-range orbiter concept. (See refs. 1 and 2.) The general arrangement of the model is shown in figure 2; afterbody details and vertical-tail descriptions are presented in figure 3. A photograph of the model is presented in figure 4. The model had a leading-edge sweep of 67.5°, interchangeable tip fins having roll-out angle varied from the original 15° to 90°, and a removable center-line vertical tail. Elevon surfaces provided both pitch and roll control and rudders on the tip fins provided directional control.

Model component designations are defined as follows:

B	basic body
B_2	body with all boattailing removed
B_3	body with side boattailing removed
W	basic wing
W_2	wing with extended trailing edge
V_1	basic tip fins
V_2	center-line vertical tail
V_3	tip fins in aft position

APPARATUS AND METHODS

The tests were conducted in the Langley low-turbulence pressure tunnel, which is a variable-pressure, single-return facility having a closed test section 0.91 meter (3.0 feet) wide and 2.3 meters (7.5 feet) high. The tunnel can accommodate tests in air at Reynolds numbers up to approximately 49.2×10^6 per meter (15.0×10^6 per foot) at Mach numbers up to about 0.40.

TEST CONDITIONS

The present investigation was made at a Reynolds number, based on body length, of 17×10^6 and at a Mach number of 0.25. The angle of attack varied from about -4° to

22°. Sideslip data were measured at a sideslip angle of 0° and -6°. All tests were made with the model in a smooth condition.

MEASUREMENTS AND CORRECTIONS

The drag coefficients presented represent gross drag in that base drag has not been subtracted. Balance cavity pressure measured during the tests is presented in part (c) of figures 5 to 12. The data have been corrected for blockage and lift interference by the methods of references 3 and 4. Angles of attack have been corrected for the effect of balance and sting deflections due to aerodynamic loads.

RESULTS AND DISCUSSION

The basic longitudinal and lateral aerodynamic characteristics of the model have been presented in references 1 and 2. The present investigation was undertaken to examine modifications to the configuration directed toward improvements in the subsonic characteristics. The previous tests (refs. 1 and 2) indicated that an interaction between the wing vortex and the tip fins resulted in rearward concentration of lift causing the model to have a very large negative $C_{m,o}$. In the present investigation modifications such as removing the tip fins and using a center vertical tail, increasing the roll-out angle of the tip fins, moving the fins aft, and alterations to the afterbody and wing trailing edge were tested to determine the effect on the stability and performance of the configuration.

Static Longitudinal Stability and Control

Effect of vertical-tail configuration.- The longitudinal aerodynamic characteristics of the model with tip fins, center tail, and combination tip fins and center tail are presented in figure 5. These data are presented with the elevons deflected -30°, which gives trim conditions close to those required for the landing attitude of 15°. The data show a slight increase in the zero-lift pitching moment and a decrease in the stability level for the center-tail configuration. This indicates a smaller trim-drag penalty and therefore an increased trimmed L/D.

Aerodynamic characteristics for center-tail configuration.- Presented in figure 6 are the longitudinal control effectiveness data for the center-tail configuration. The data show that an elevon deflection of -20° is sufficient to trim the model up to the landing attitude (15°) with a maximum untrimmed L/D of 4.7. These data also show that the model is essentially neutrally stable at angles of attack up to approximately 8° with a stable break in the curve at the higher angles.

Aerodynamic characteristics of the tip-fin configuration.- The effect on the longitudinal characteristics of increasing the fin roll-out angle (see fig. 3(d)) from the original angle (15^o) up to 60^o with $\delta_e = 0^o$ is shown in figure 7 and up to 90^o with $\delta_e = -30^o$ in figure 8. These data were obtained for the configuration with body B_3. These tests were made in an attempt to eliminate the large negative $C_{m,o}$. The data show only a very small change in $C_{m,o}$ and, as expected, there was a large increase in the longitudinal stability with increased roll-out angle. These results indicate that for the same center-of-gravity location the increased stability resulted in an increase in the trim-drag penalty and therefore would result in a lower trimmed L/D.

Presented in figures 9 and 10 are data showing the effects of moving the tip fins aft (see fig. 3(d)) on the longitudinal characteristics of the model with body B_3. Figure 9 is for the configuration with $\delta_e = 0^o$ and figure 10 is for the configuration with $\delta_e = -30^o$. These data show that moving the fins aft resulted in a decrease in longitudinal stability with little change in the negative $C_{m,o}$ and thereby resulted in very little change in trimmed L/D.

Aerodynamic characteristics with extended trailing edge.- In an attempt to improve the subsonic characteristics of the center-tail configuration, the model was tested with the wing trailing edge extended as shown in figure 3(b). The data presented in figure 11 show that the model was slightly unstable up to about an angle of attack of 6^o and slightly stable above this angle of attack. An elevon deflection of only -10^o was required to trim the model up to near landing attitude. This indicates a very small trim-drag penalty and possibly an improved trimmed L/D.

Aerodynamic characteristics with boattailing removed.- The data of figure 12 present the elevon effectiveness of the model with the boattailing of the body removed. (See fig. 3(b).) Removing the body boattailing had little effect on the longitudinal stability of the model but it did reduce the negative $C_{m,o}$ to about one-half of its original value. This decreased value of $C_{m,o}$ indicates a decrease in the trim-drag penalty; however, the increased base area would offset the associated increase in L/D.

Longitudinal trim characteristics.- Figure 13 summarizes the longitudinal trim characteristics of the model with three of the modifications previously discussed. The data, presented for a center of gravity located at 66.7 percent of the body length, show that removing the tip fins and adding a center vertical tail increased the maximum trimmed L/D from approximately 3.4 to 5.1. Extending the wing trailing edge on the model with the center-tail configuration resulted in a small additional increase to 5.3. Removing the boattailing from the afterbody of the center-tail configuration reduced the negative $C_{m,o}$ by one-half but also decreased the maximum trimmed L/D by about 0.6.

Static Lateral-Directional Stability Characteristics

Basic model.- The static lateral-directional stability characteristics of the model are presented in figure 14. The data presented for the model with the elevons undeflected (obtained from ref. 1) show that the model is directionally stable $\left(+C_{n_\beta}\right)$ only up to an angle of attack of about 14° with positive dihedral effect $\left(-C_{l_\beta}\right)$ throughout the test angle-of-attack range. Tests of the present investigation show that deflecting the elevons -30° (required for trim) resulted in a large increase in C_{n_β} at the higher angles of attack and thus caused the model to be stable directionally throughout the test angle-of-attack range.

Effect of vertical tail configuration.- Presented in figure 15 are data comparing the basic wing-body configuration with tip-fin and center-tail configurations with the elevons deflected -30°. The data show the wing-body to be unstable; however, the stabilizing increments of the center tail and tip fins are about the same. There was a larger variation in C_{l_β} with angle of attack for the tip-fin configurations.

The data of figure 16 indicate the effect of tip-fin roll-out angle on the lateral-directional characteristics of the model. These data show that as the roll-out angle is increased from 15° to 90° there is a decrease in the directional stability until at 60° and 90° the model is unstable throughout the test angle-of-attack range. Data presented in figure 17 show that, as expected, moving the fins aft increased the directional stability throughout the test angle-of-attack range.

SUMMARY OF RESULTS

An investigation of several configuration modifications to improve the subsonic aerodynamic performance of a blended delta wing-body space shuttle-orbiter concept has been conducted in the Langley low-turbulence pressure tunnel. The results of the tests on a 0.013-scale model of the vehicle may be summarized as follows:

1. Removing the tip fins and adding a center vertical tail increased the maximum trimmed lift-drag ratio from approximately 3.4 to 5.1 with no change in the trimmed lift coefficient for the model with the center of gravity at 66.7 percent of the body length.

2. Extending the wing trailing edge on the model with the center-tail configuration resulted in an increase in the maximum trimmed lift-drag ratio to 5.3.

3. Removing the boattailing from the afterbody of the model with the center-tail configuration reduced the negative pitching moment at zero lift by one-half, but also decreased the maximum trimmed lift-drag ratio by about 0.6.

4. Deflecting the elevons to -30° on the model with the tip-fin configuration increased the directional stability significantly at the high angles of attack and thus caused the model to be stable throughout the test angle-of-attack range.

5. The subsonic directional stability characteristics of both the tip-fin and the center-tail configurations are similar.

Langley Research Center,
National Aeronautics and Space Administration,
Hampton, Va., January 6, 1972.

REFERENCES

1. Freeman, Delma C., Jr.: Low-Subsonic Aerodynamic Characteristics of a Space Shuttle-Orbiter Concept With a Blended Delta Wing-Body. NASA TM X-2209, 1971.
2. Fox, Charles H., Jr.; and Freeman, Delma C., Jr.: Subsonic Stability, Control, and Performance of a Shuttle Concept With a Blended Wing-Body. NASA TM X-2341, 1971.
3. Herriot, John G.: Blockage Corrections for Three-Dimensional-Flow Closed-Throat Wind Tunnels, With Consideration of the Effect of Compressibility. NACA Rep. 995, 1950. (Supersedes NACA RM A7B28.)
4. Garner, H. C.; Rogers, E. W. E.; Acum, W. E. A.; and Maskell, E. C.: Subsonic Wind Tunnel Wall Corrections. AGARDograph 109, 1966.

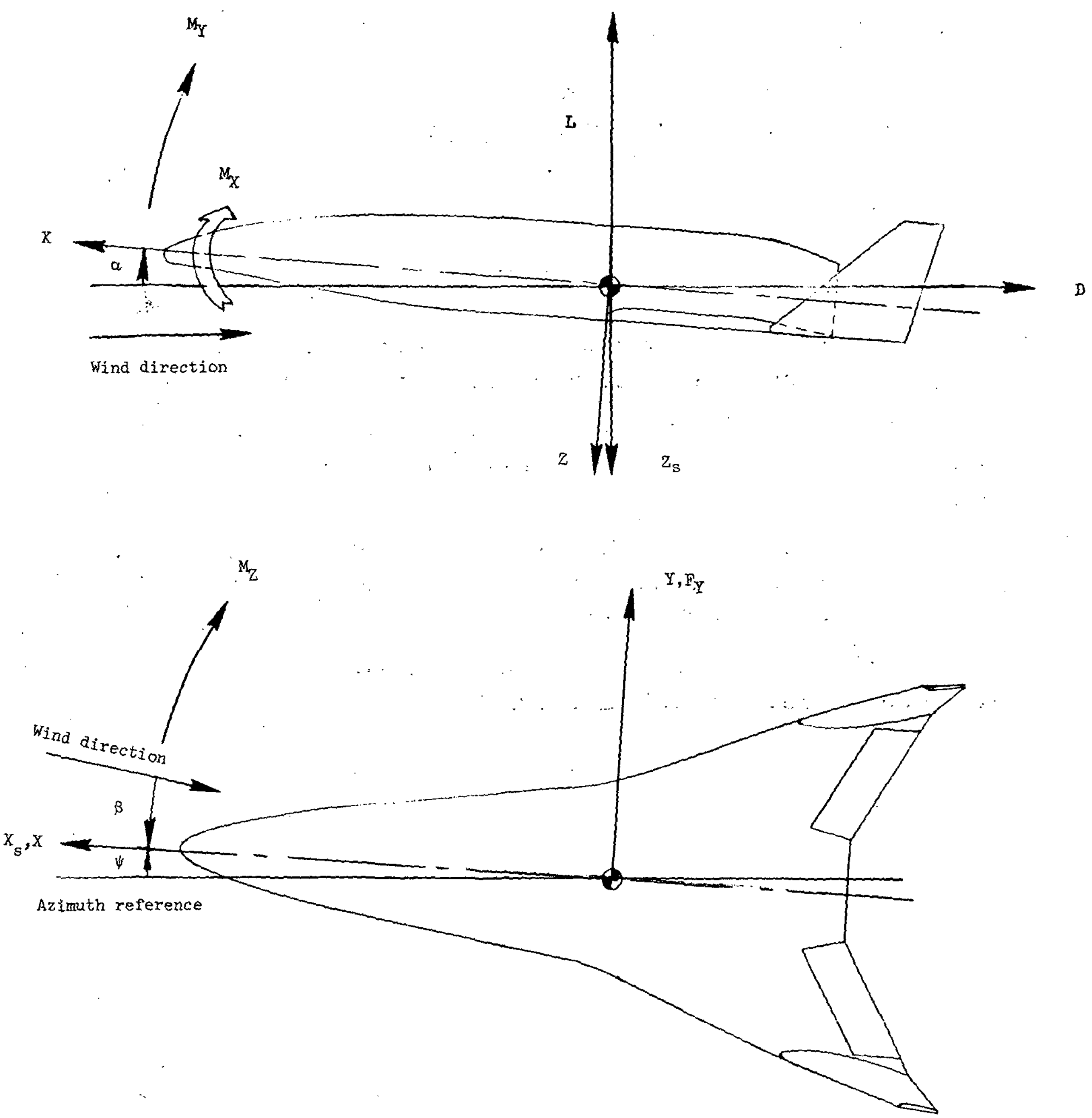

Figure 1.- System of axes used in investigation. Arrows indicate positive directions of moments, forces, and angles.

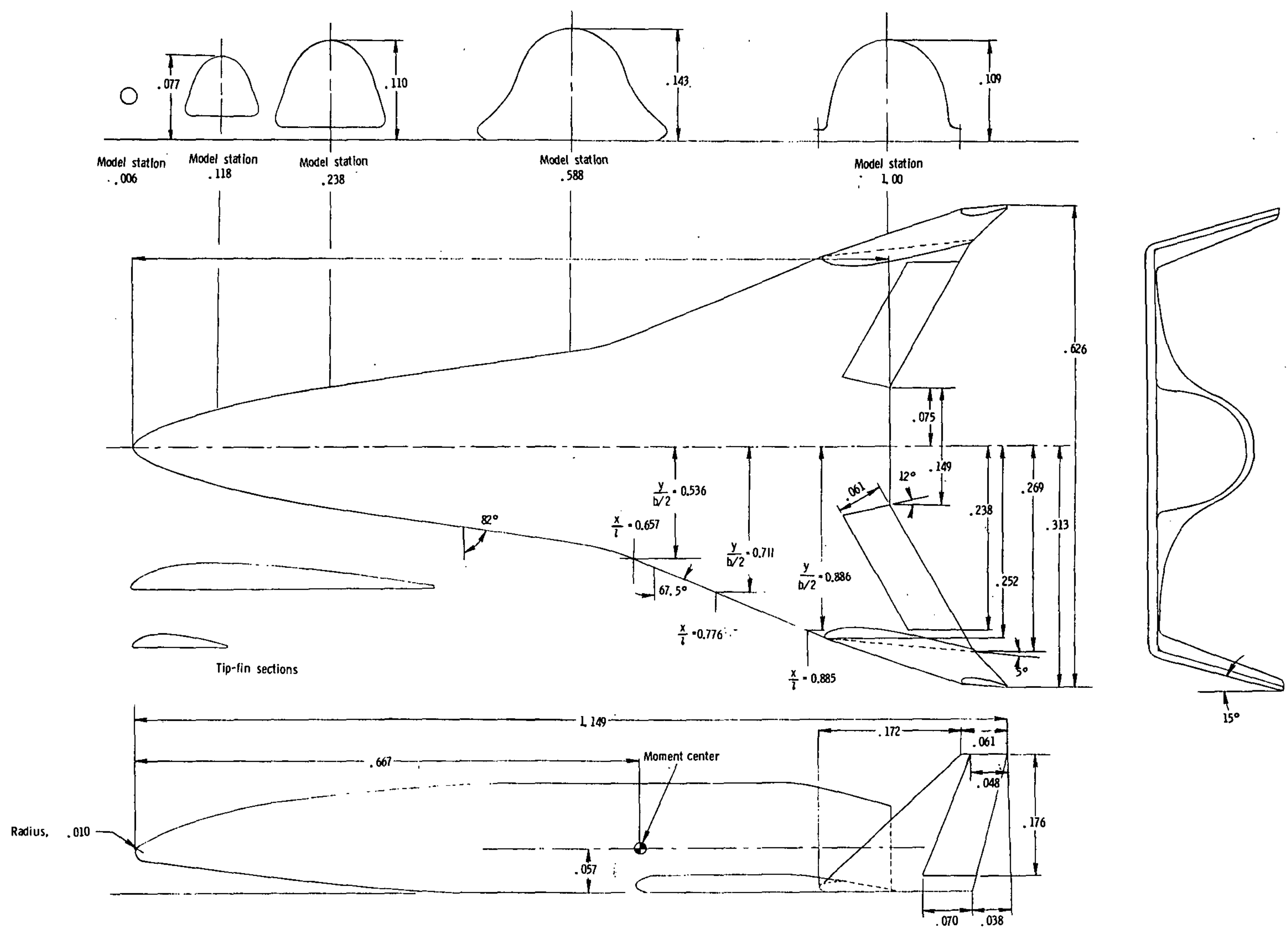

(a) Three-view drawing of model.

Figure 2.- Detail drawings of model. Linear dimensions are in percent body length; l = 66.26 cm (26.087 in.).

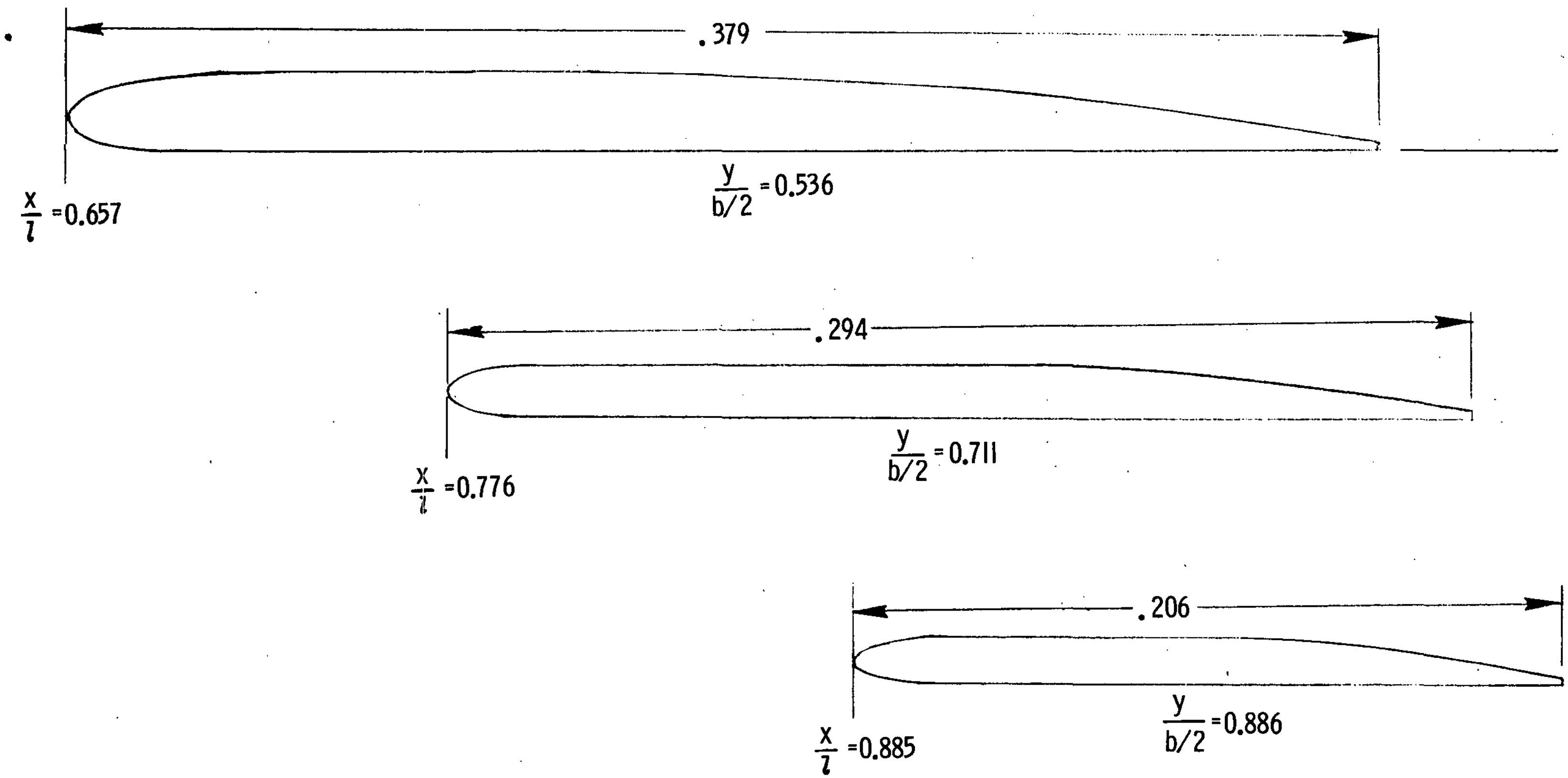

(b) Wing cross sections.

Figure 2.- Concluded.

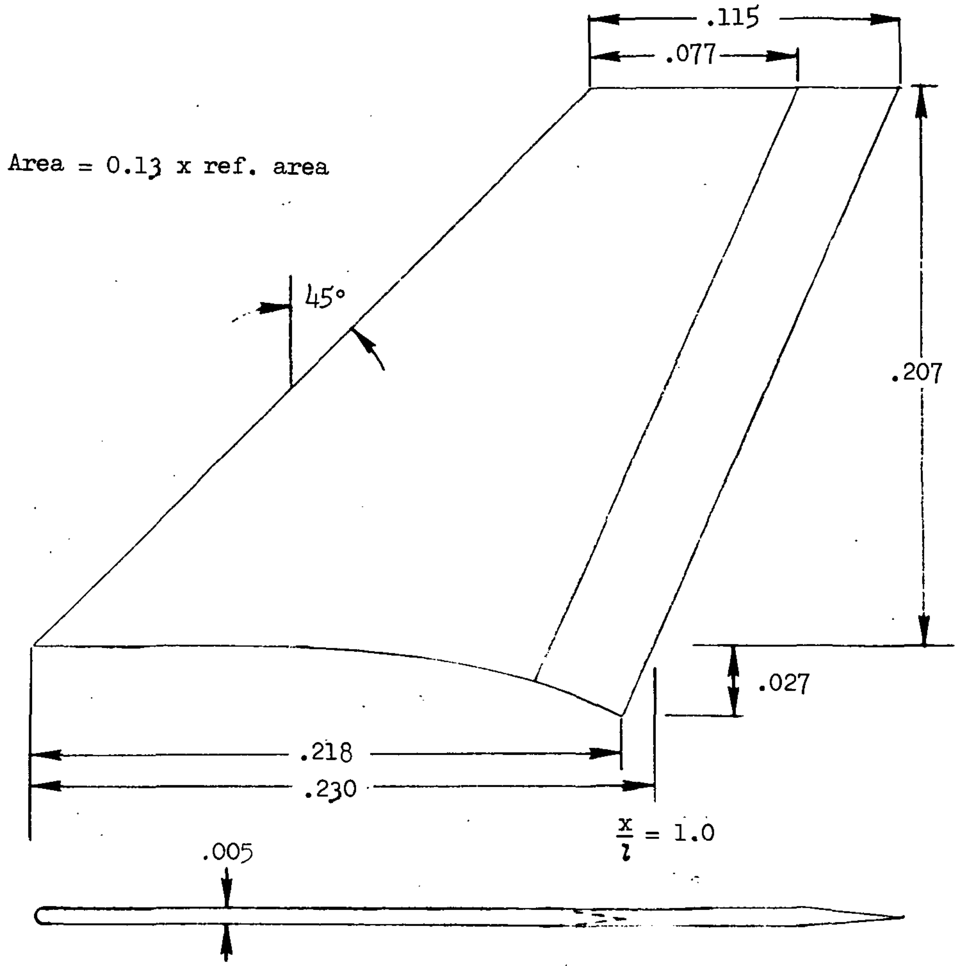

(a) Center vertical tail, V_2.

Figure 3.- Details of configuration modifications. Linear dimensions in percent body length; l = 66.26 cm (26.087 in.).

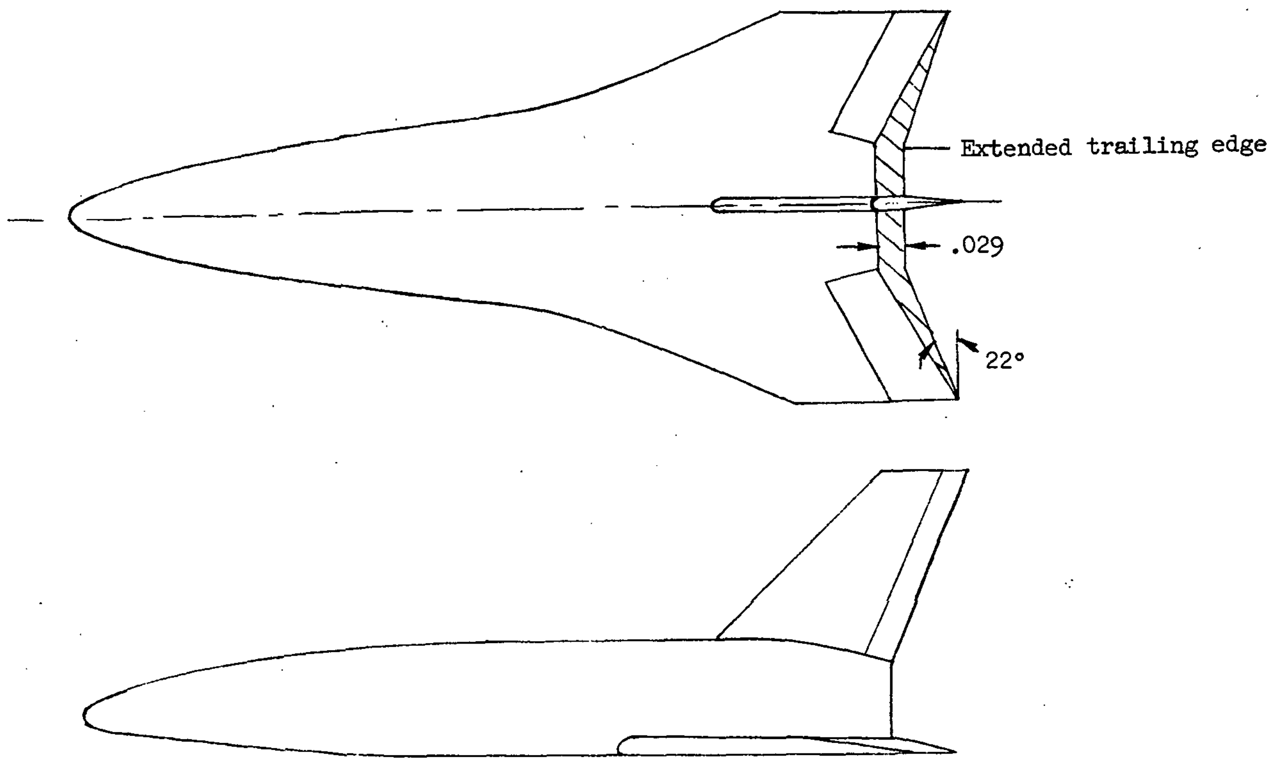

(b) Extended-trailing-edge wing, W_2.

Figure 3.- Continued.

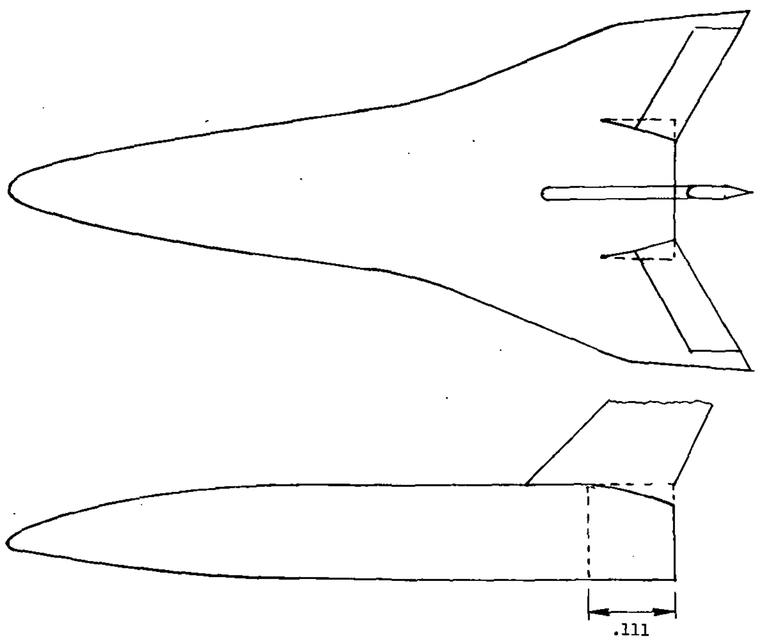

Top and side views

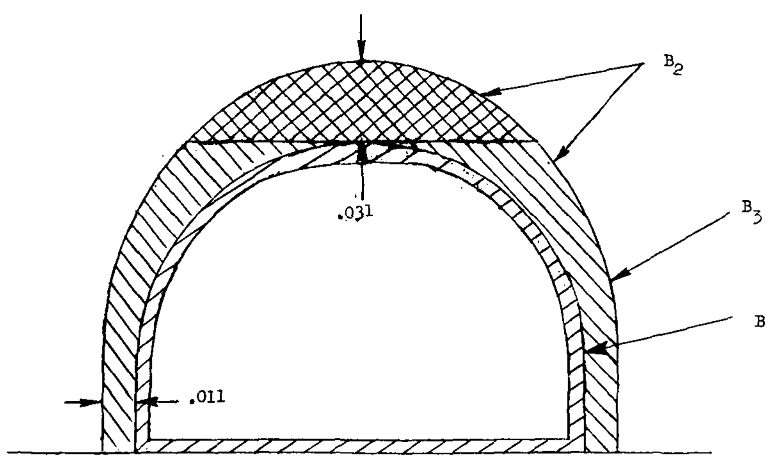

Body cross-section station, $x/l = 1.00$

(c) Body boattailing details.

Figure 3.- Continued.

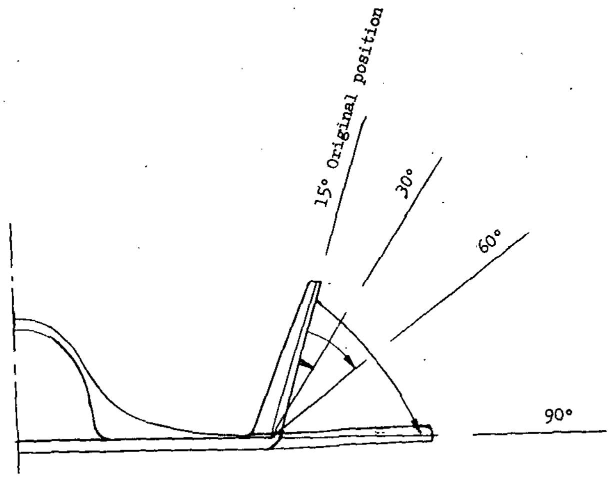

Fin roll-out

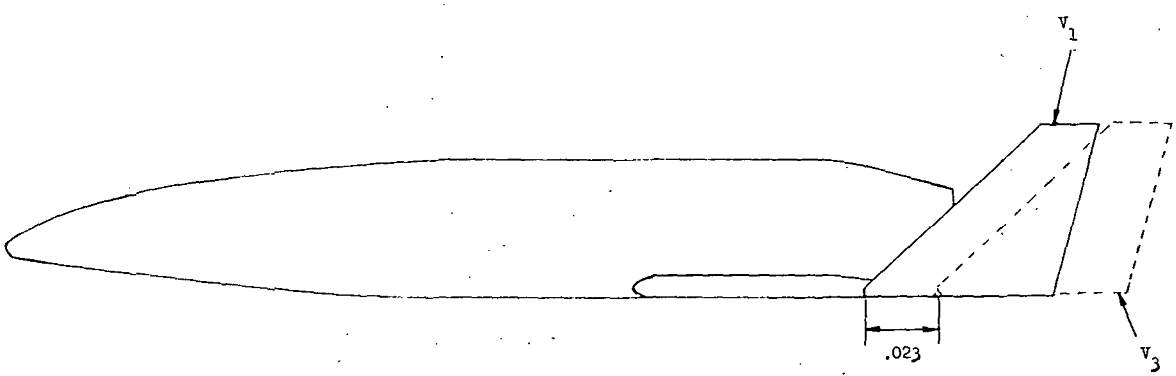

Tip-fin positions

(d) Tip-fin roll-out angle and location details.

Figure 3.- Concluded.

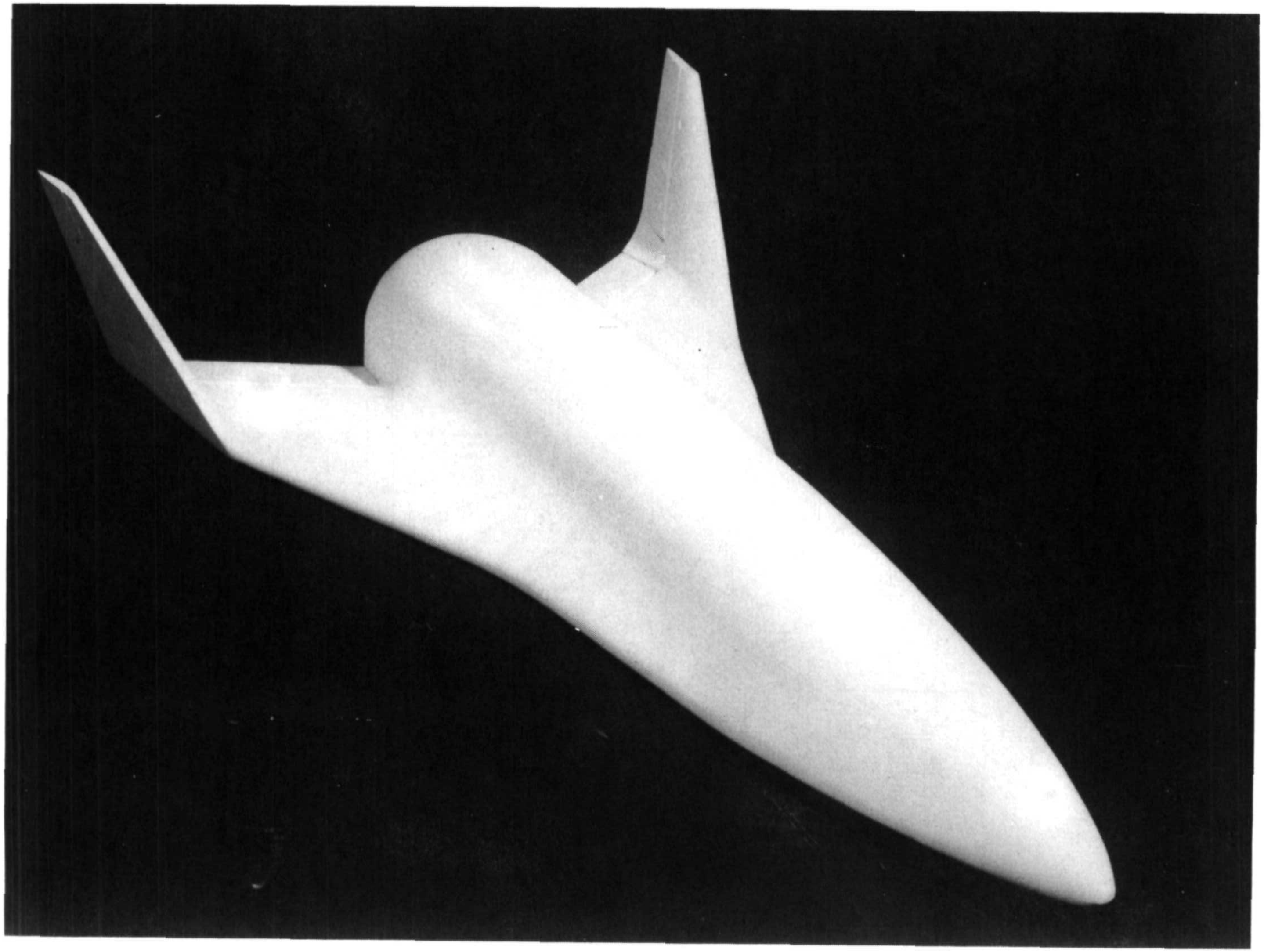

L-70-4671

Figure 4.- Photograph of model.

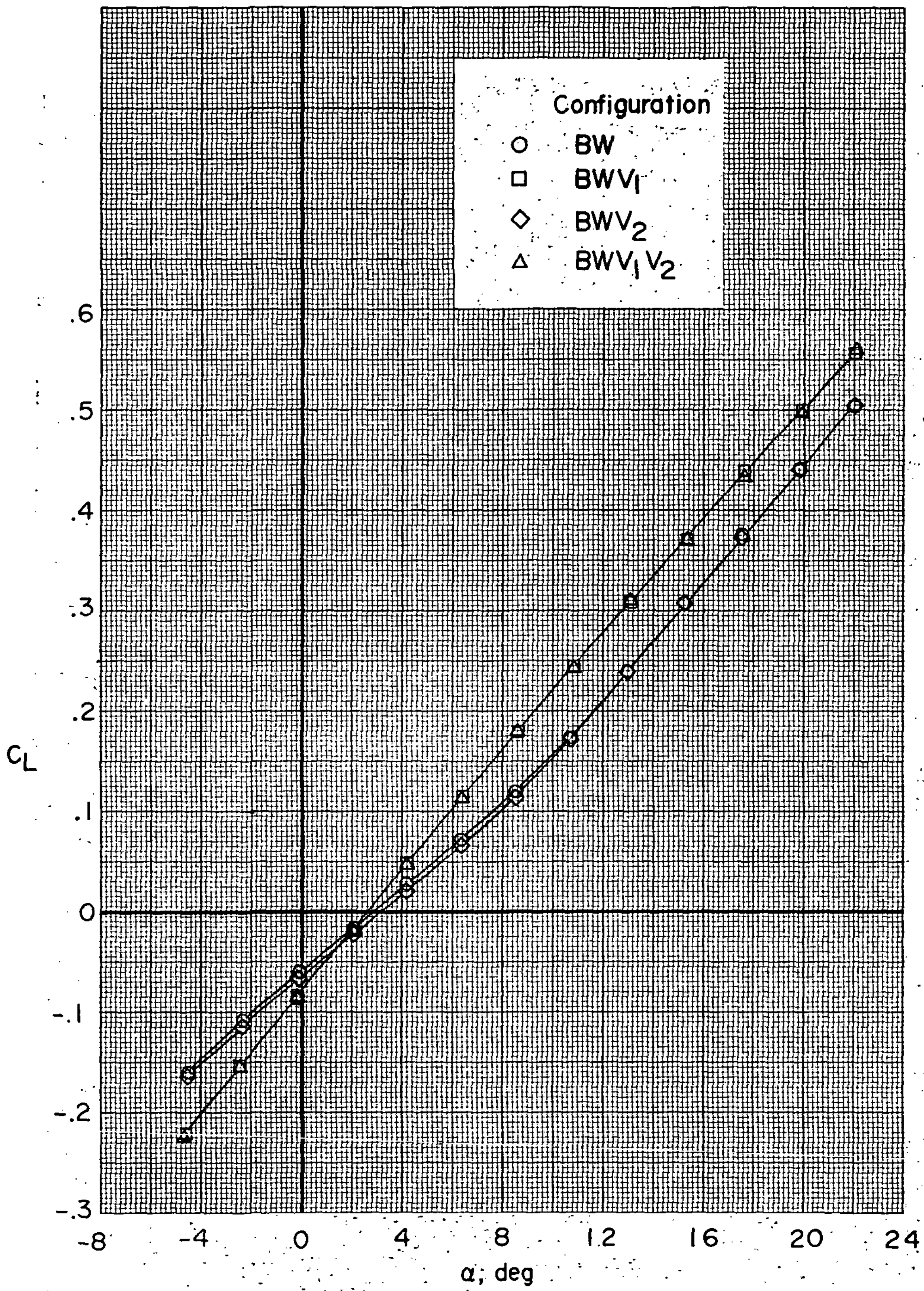

(a) C_L as a function of α.

Figure 5.- Effect of vertical tail configuration on longitudinal characteristics of model. $\delta_e = -30^{\circ}$.

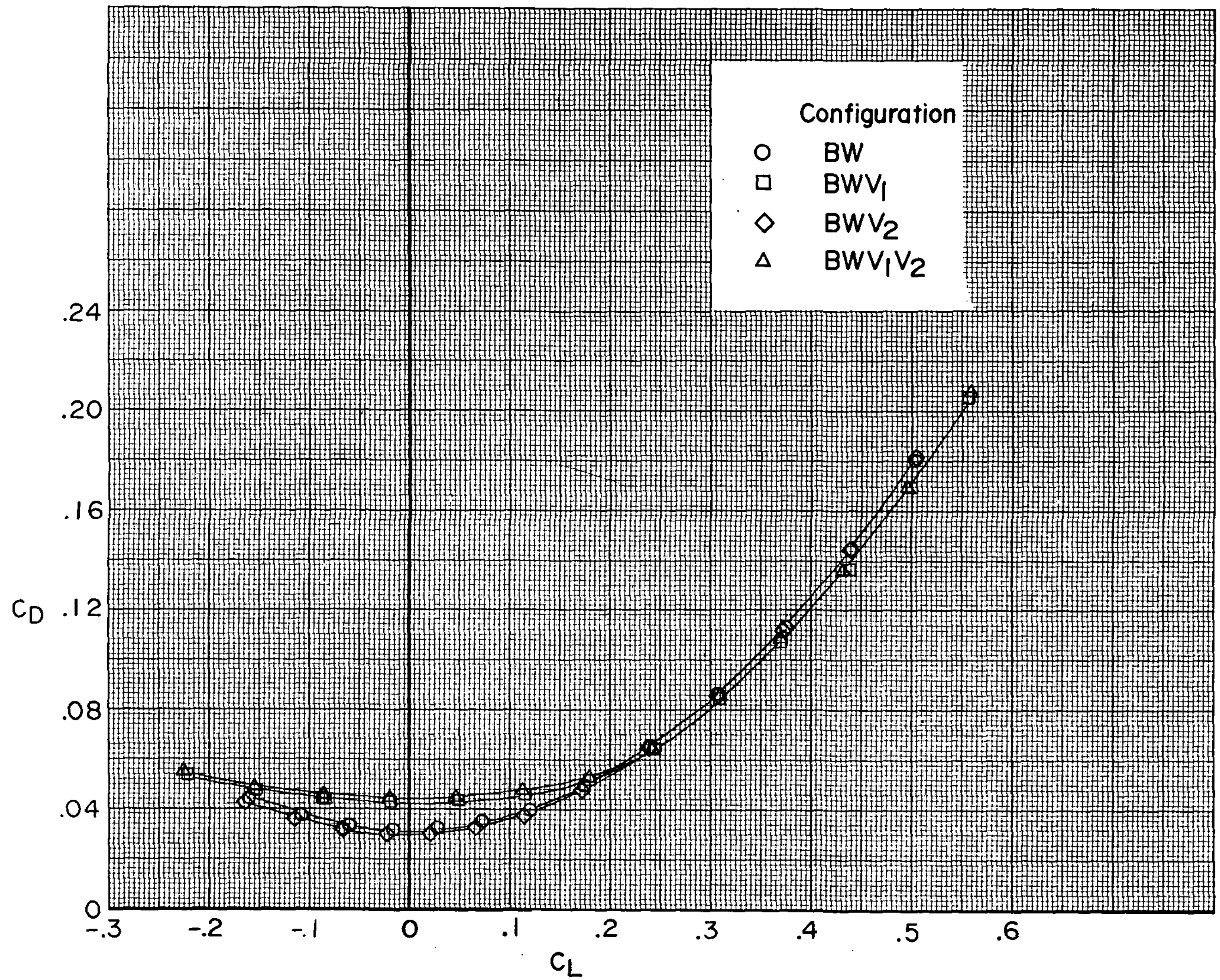

(b) C_D as a function of C_L.

Figure 5.- Continued.

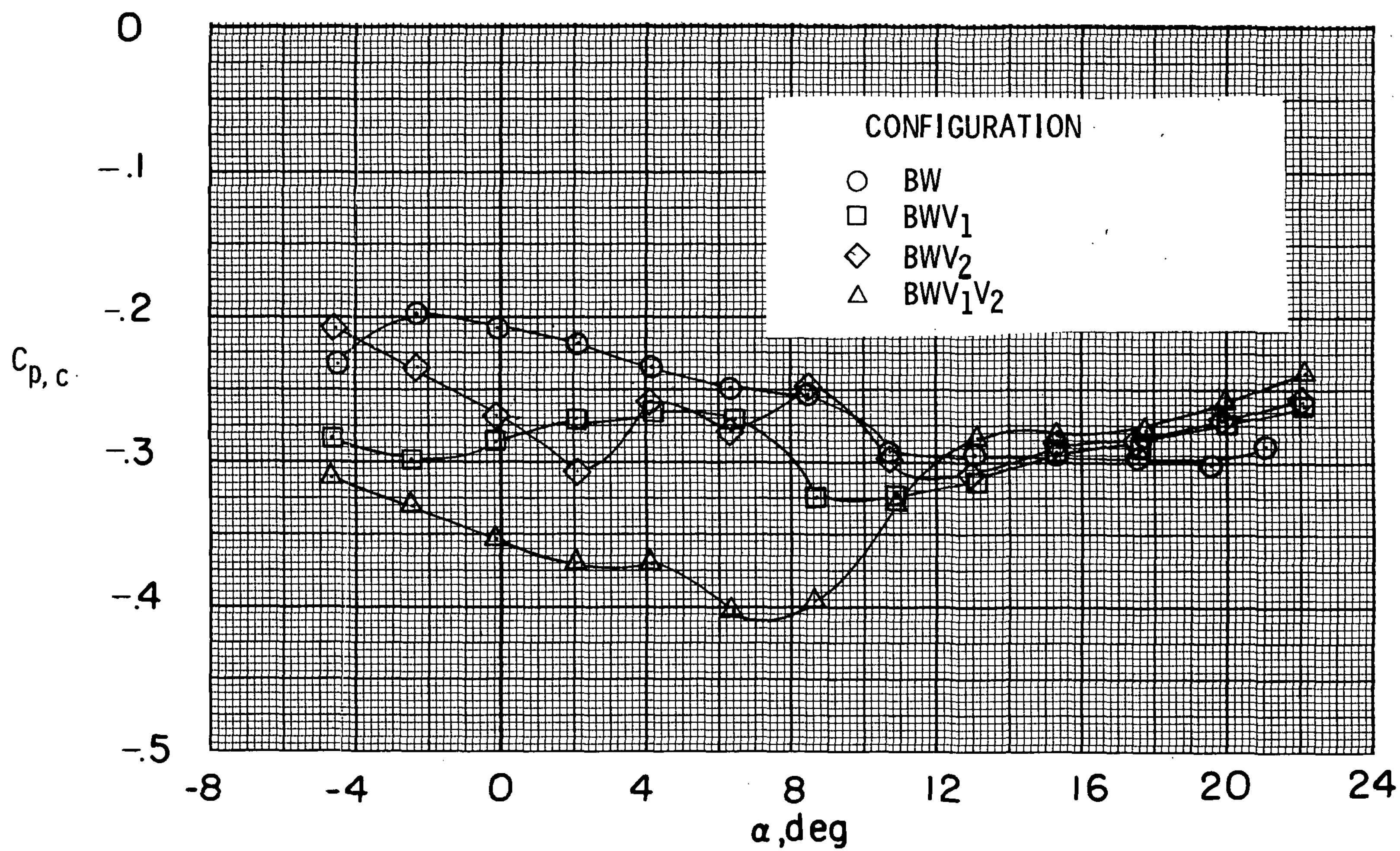

(c) $C_{p,c}$ as a function of α.

Figure 5.- Continued.

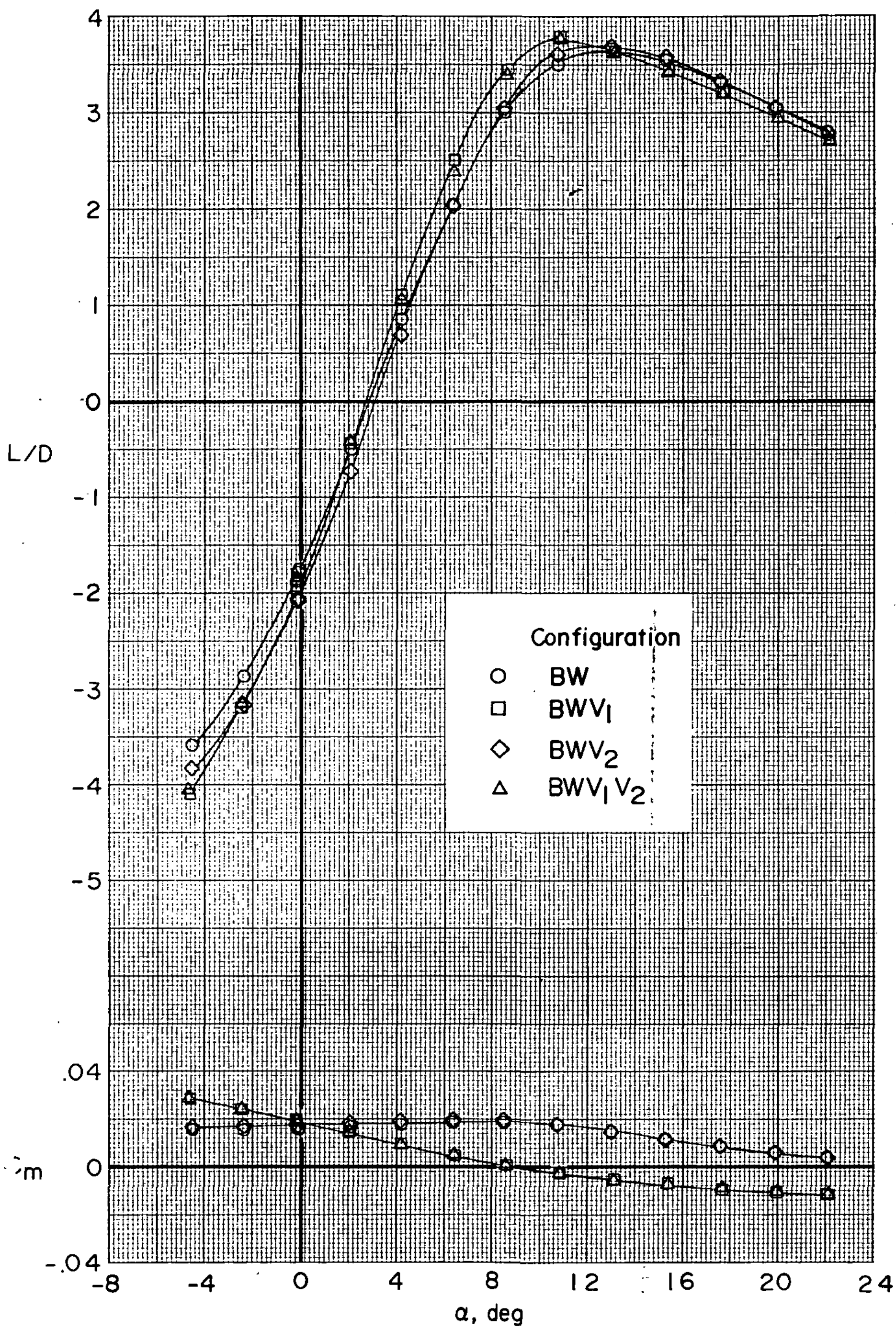

(d) L/D and C_m as a function of α.

Figure 5.- Continued.

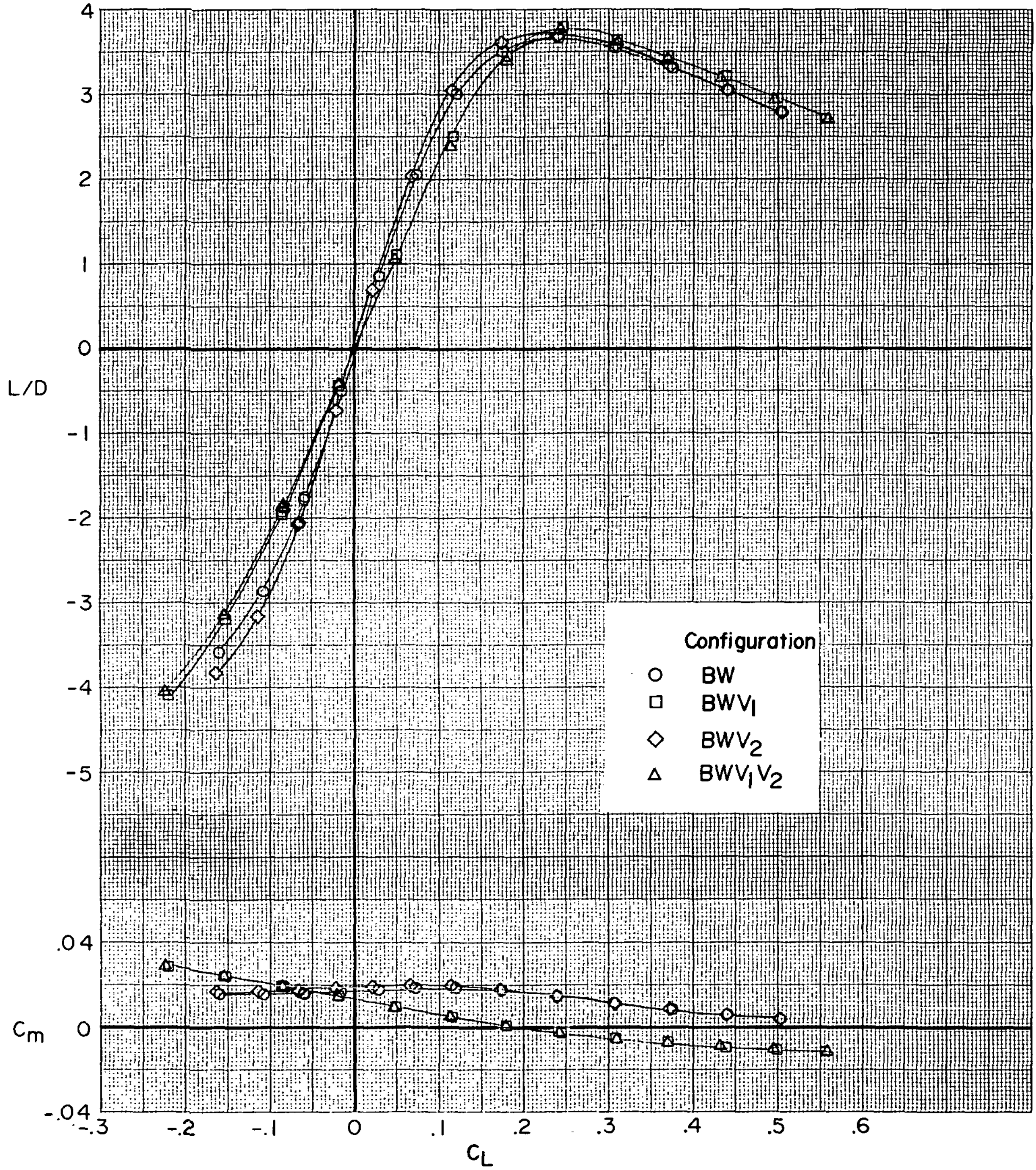

(e) L/D and C_m as a function of C_L.

Figure 5.- Concluded.

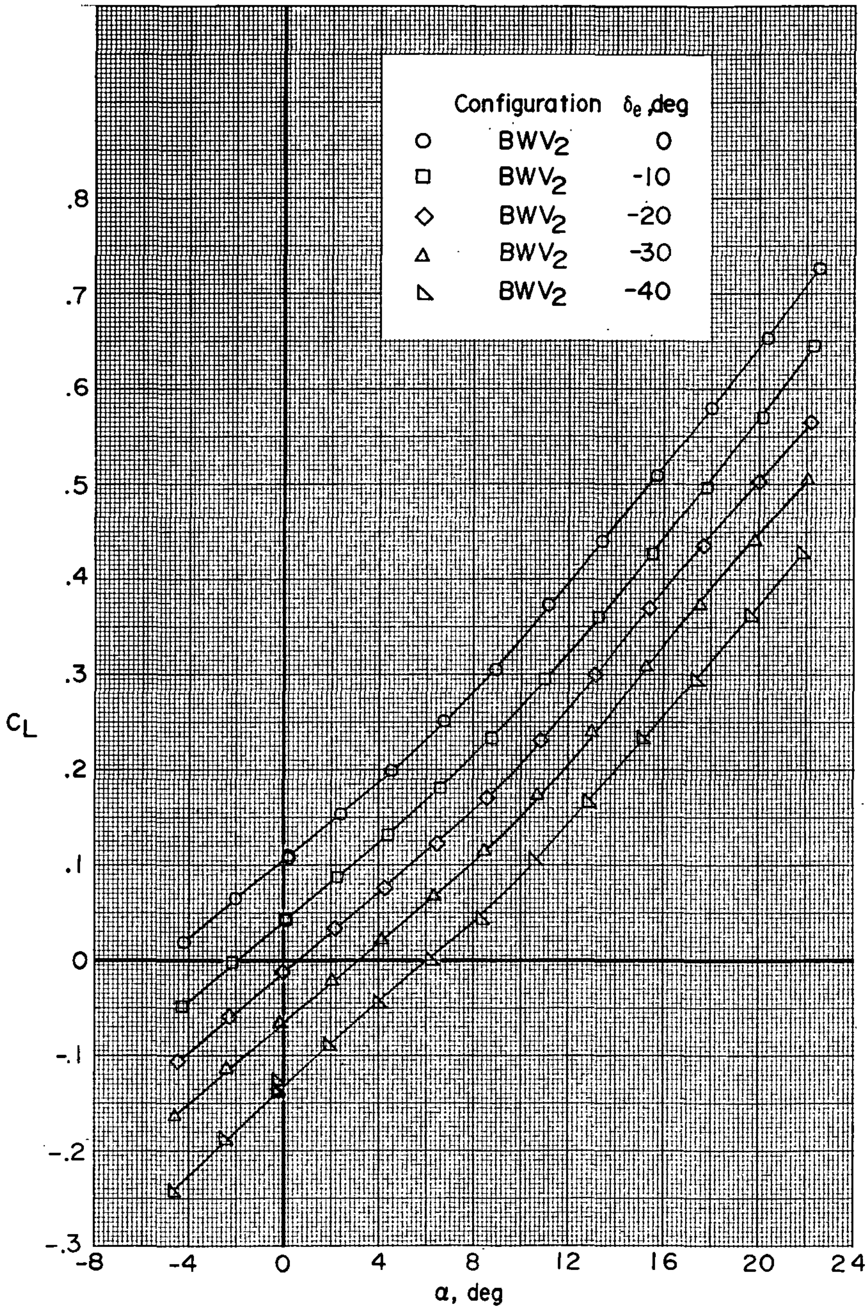

(a) C_L as a function of α.

Figure 6.- Longitudinal control effectiveness of center-tail configuration BWV_2.

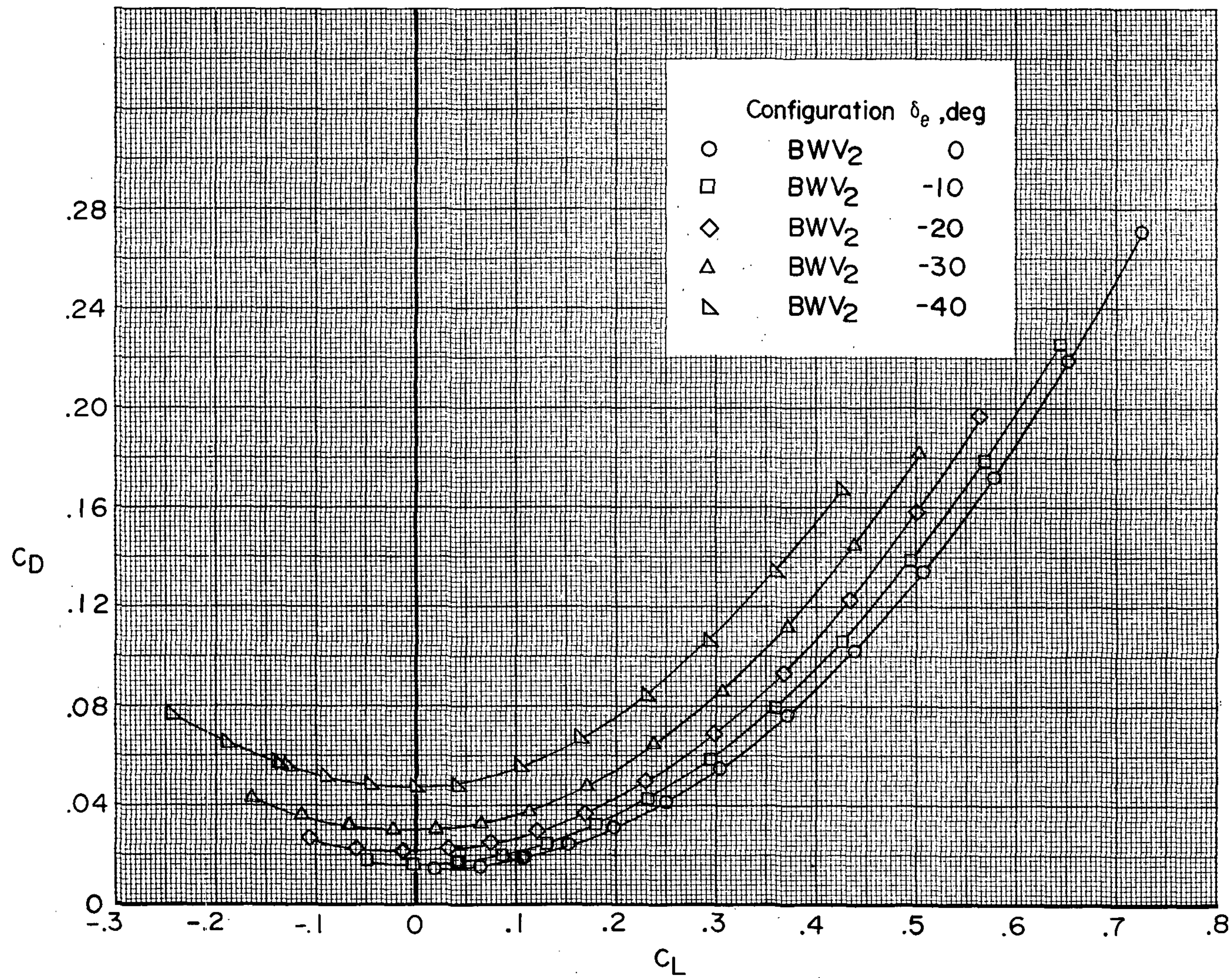

(b) C_D as a function of C_L.

Figure 6.- Continued.

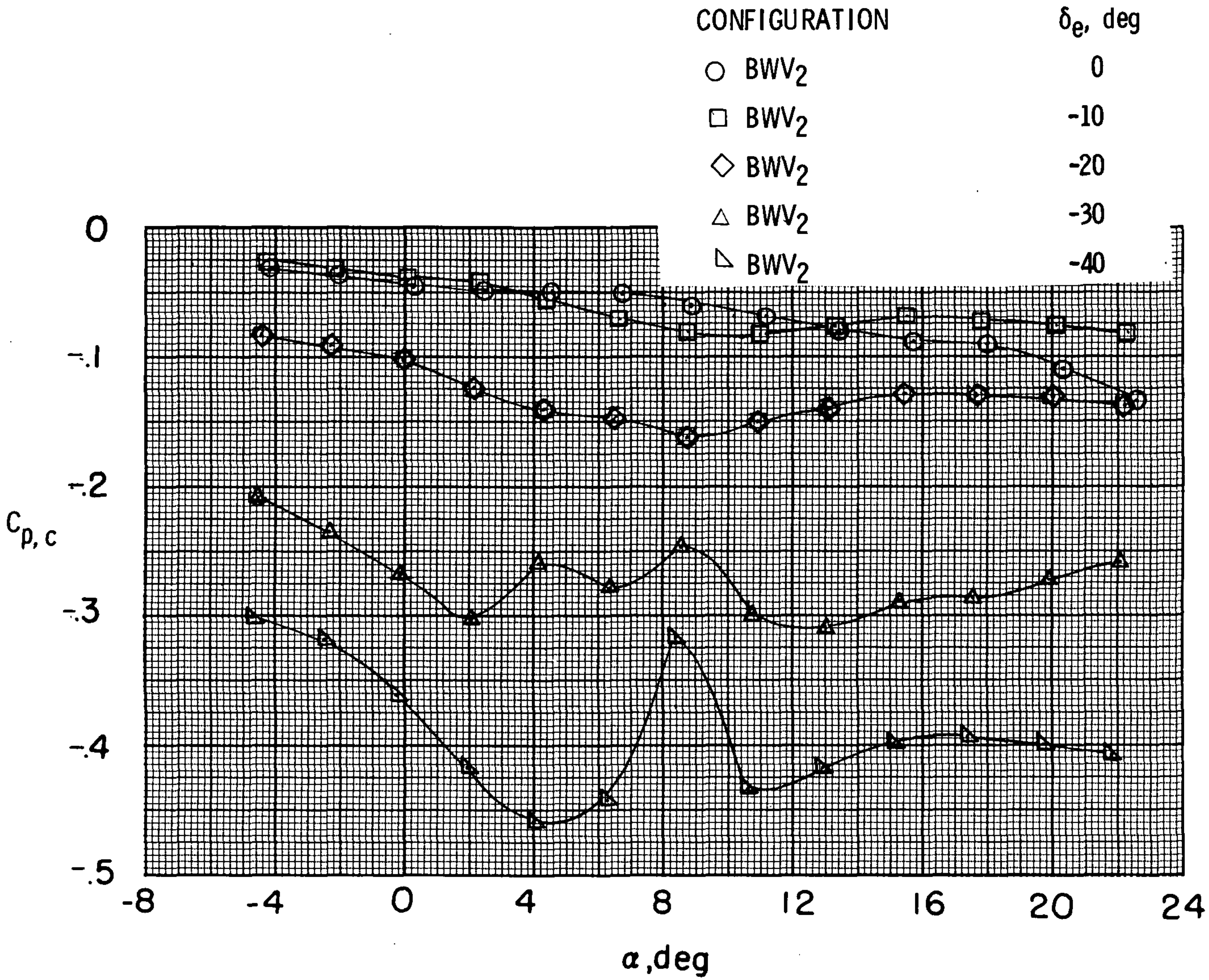

(c) $C_{p,c}$ as a function of α.

Figure 6.- Continued.

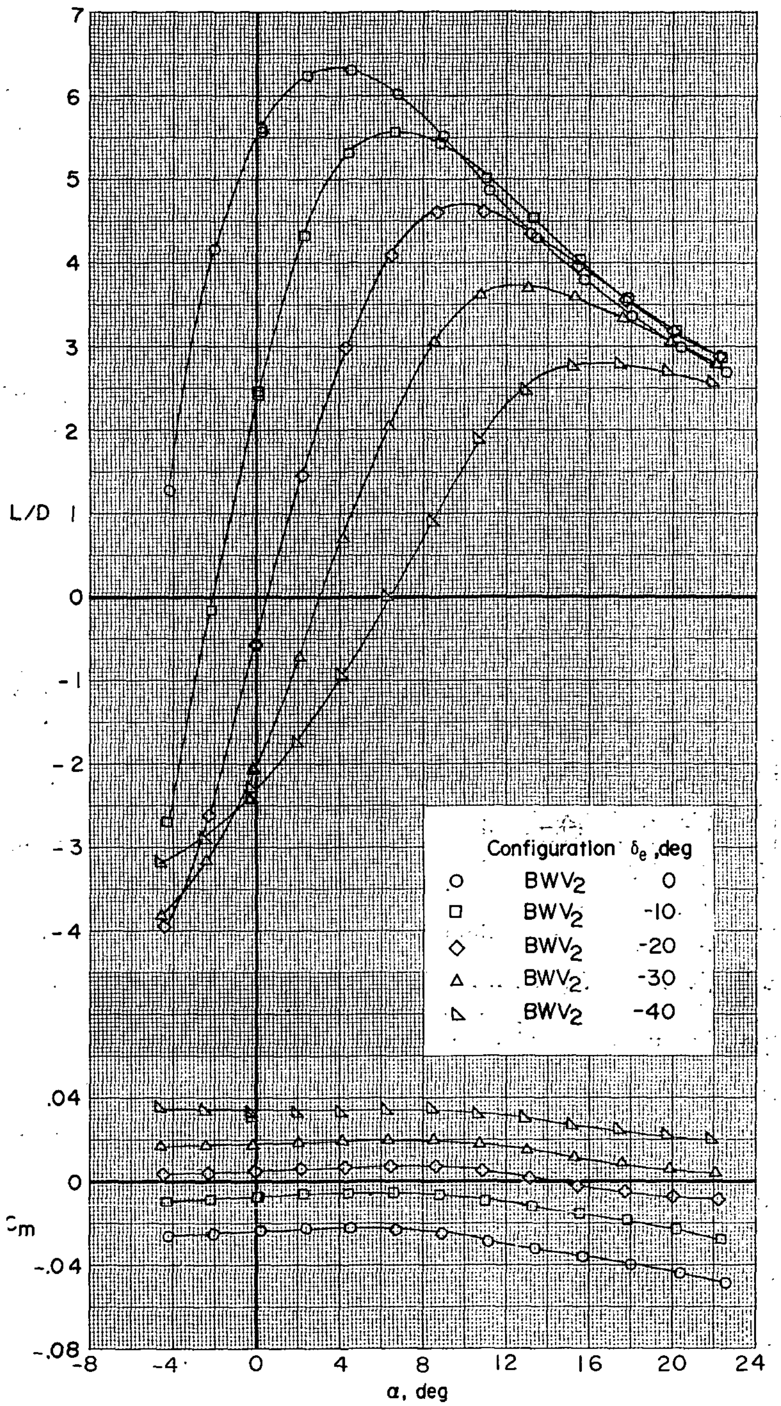

(d) L/D and C_m as a function of α.

Figure 6.- Continued.

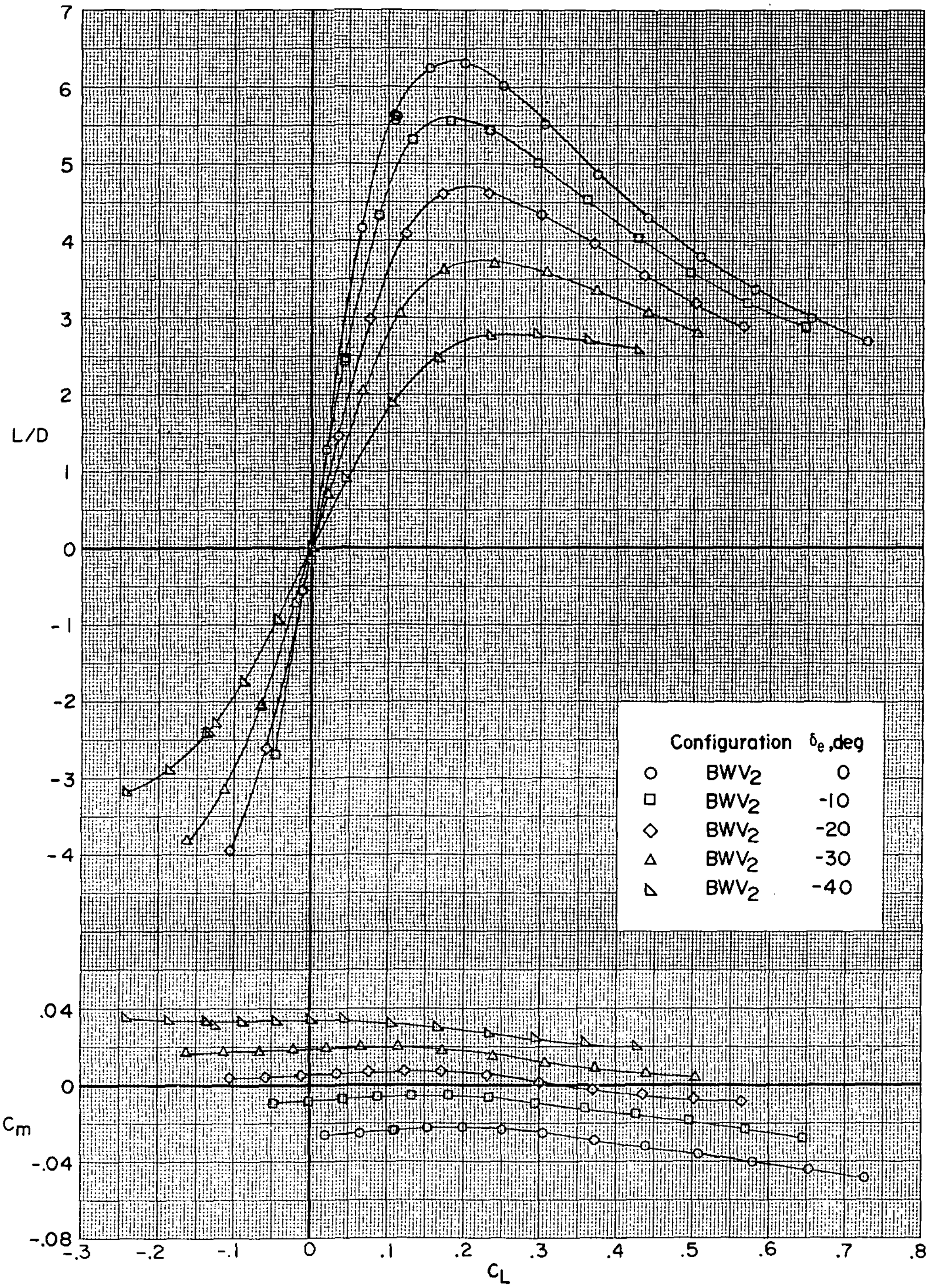

(e) L/D and C_m as a function of C_L.

Figure 6.- Concluded.

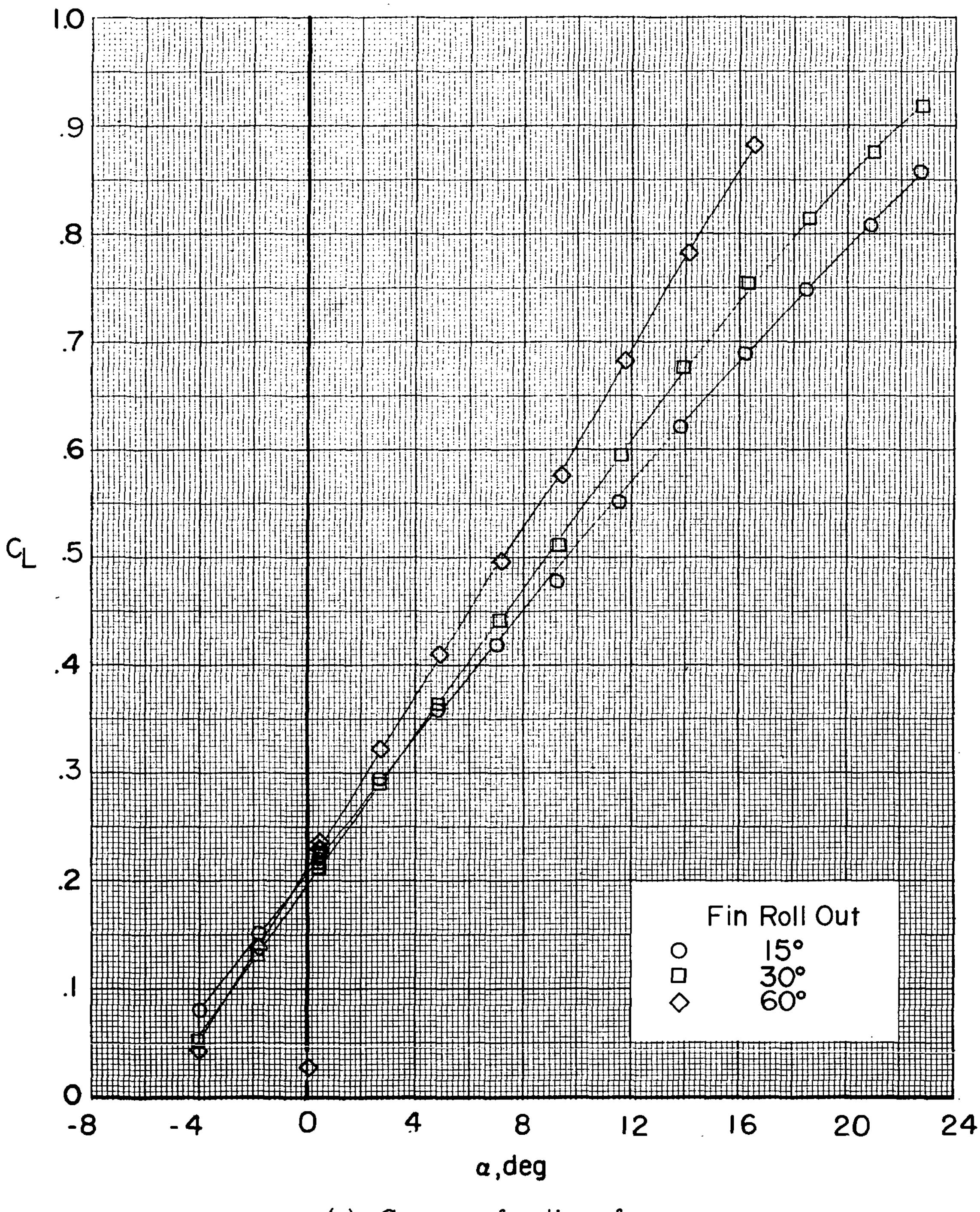

(a) C_L as a function of α.

Figure 7.- Effect of fin roll out on longitudinal characteristic of model. $\delta_e = 0^{\circ}$; configuration B_3WV_1.

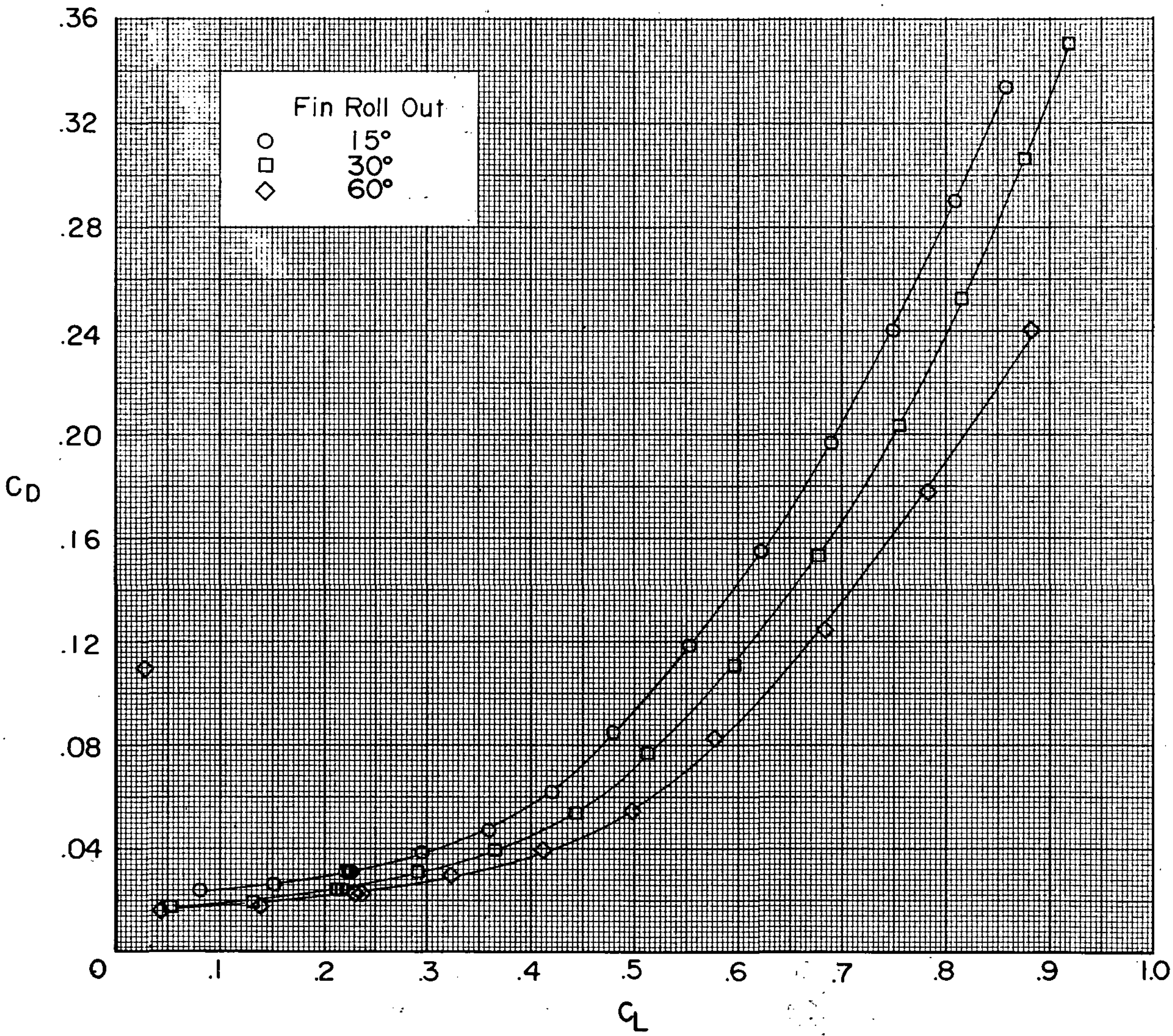

(b) C_D as a function of C_L.

Figure 27.- Continued.

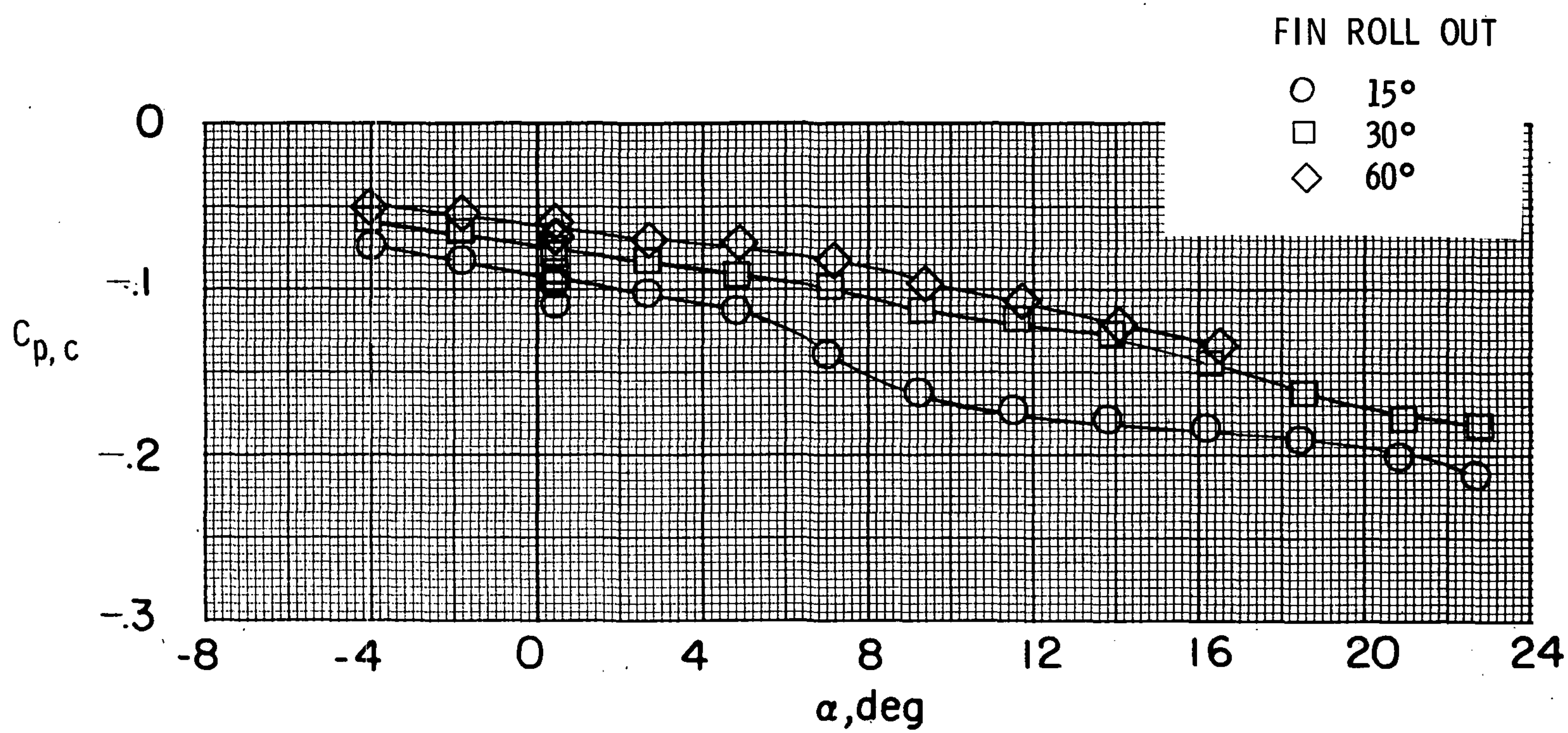

(c) $C_{p,c}$ as a function of α.

Figure 7.- Continued.

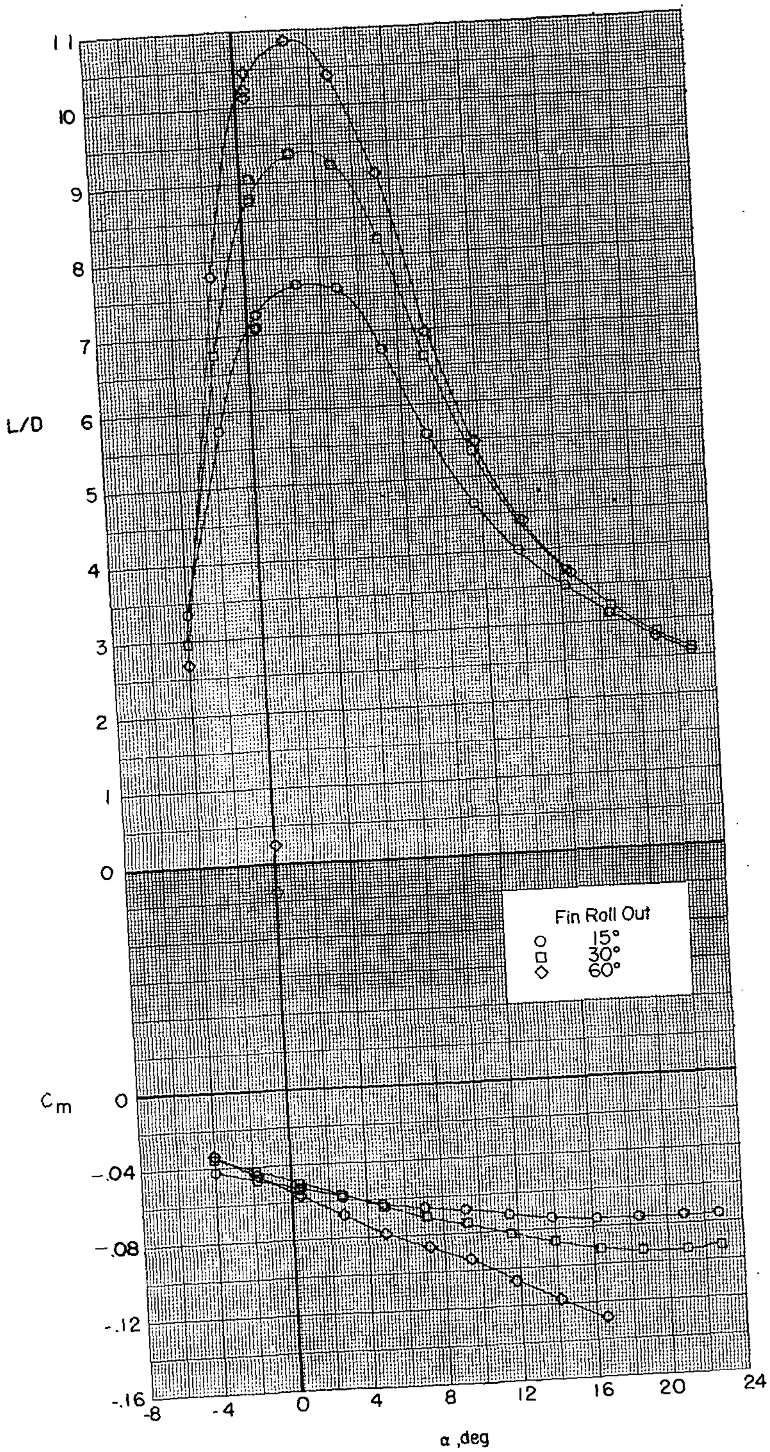

(d) L/D and C_m as a function of α.

Figure 7.- Continued.

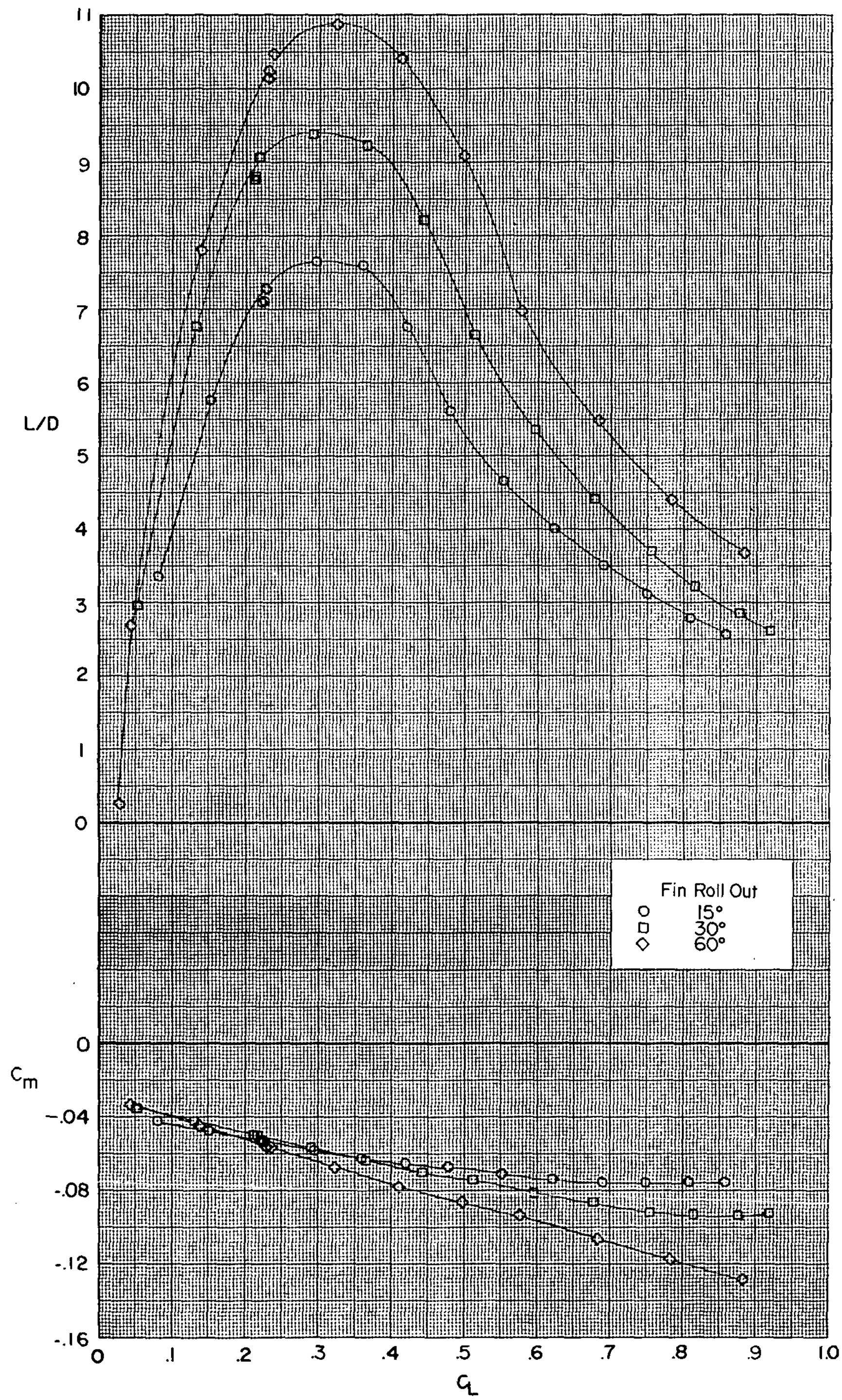

(e) L/D and C_m as a function of C_L.

Figure 7.- Concluded.

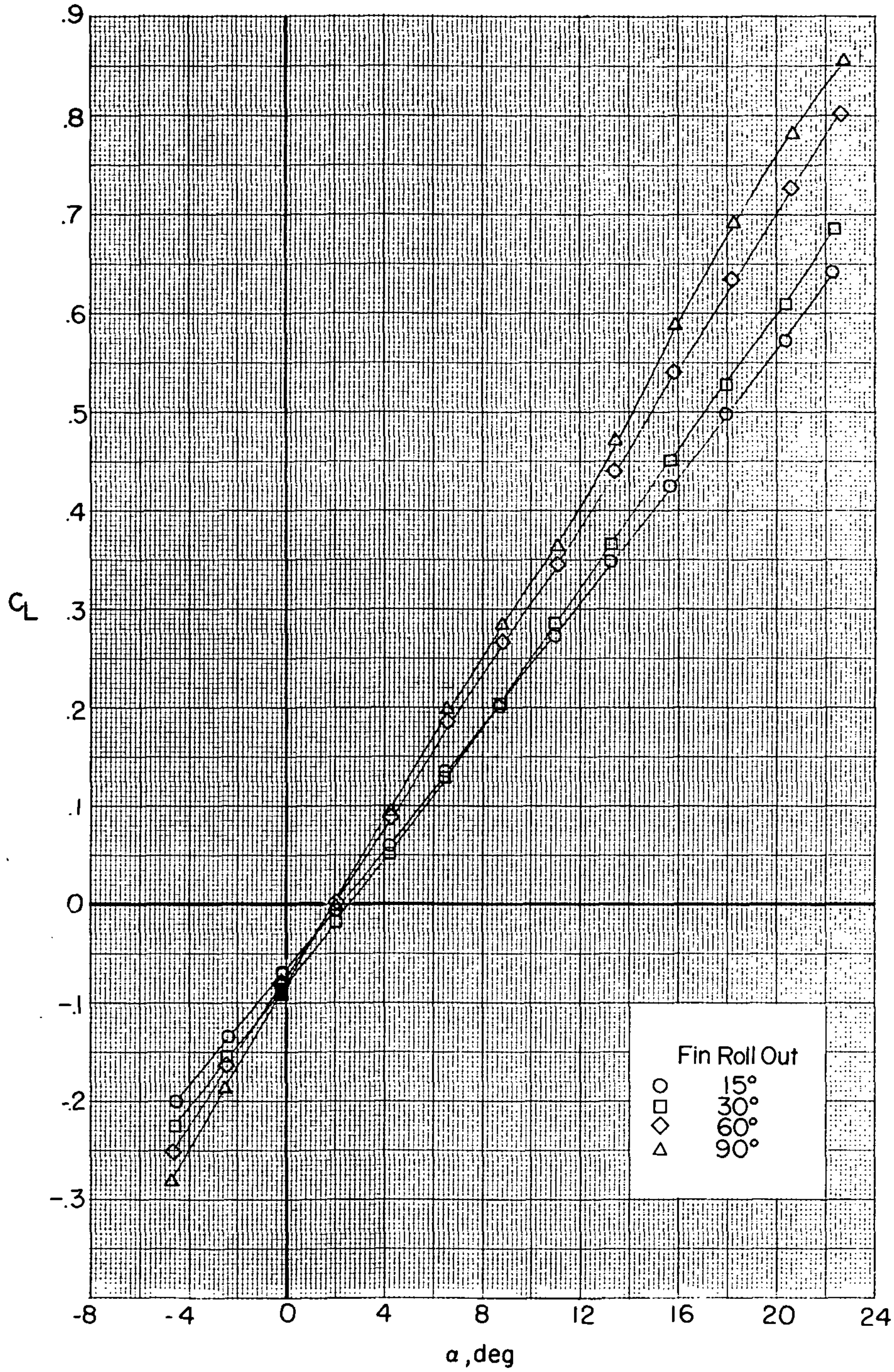

(a) C_L as a function of α.

Figure 8.- Effect of fin roll-out angle on longitudinal characteristics of model. $\delta_e = -30^{\circ}$; configuration B_3WV_1.

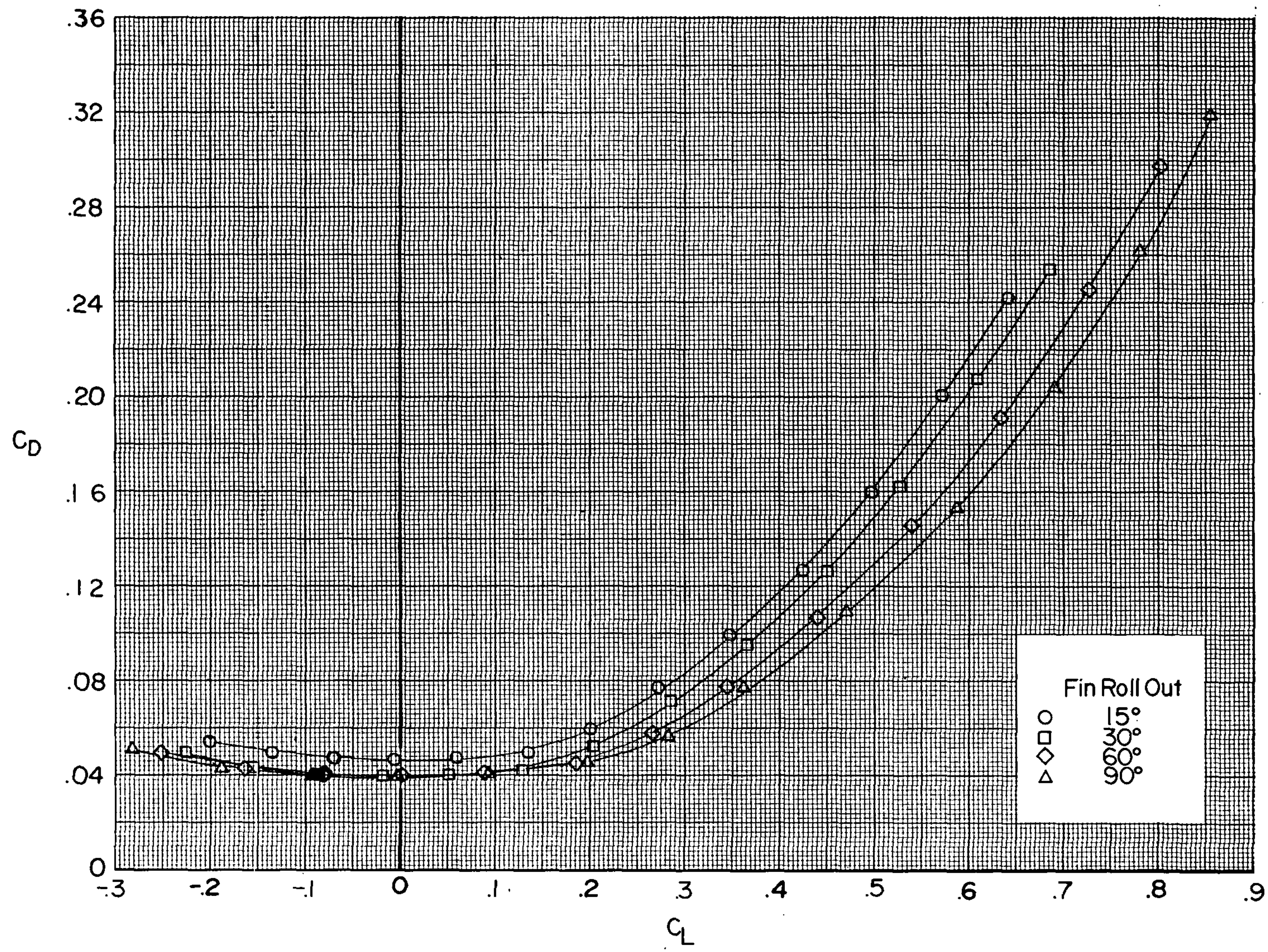

(b) C_D as a function of C_L.

Figure 8.- Continued.

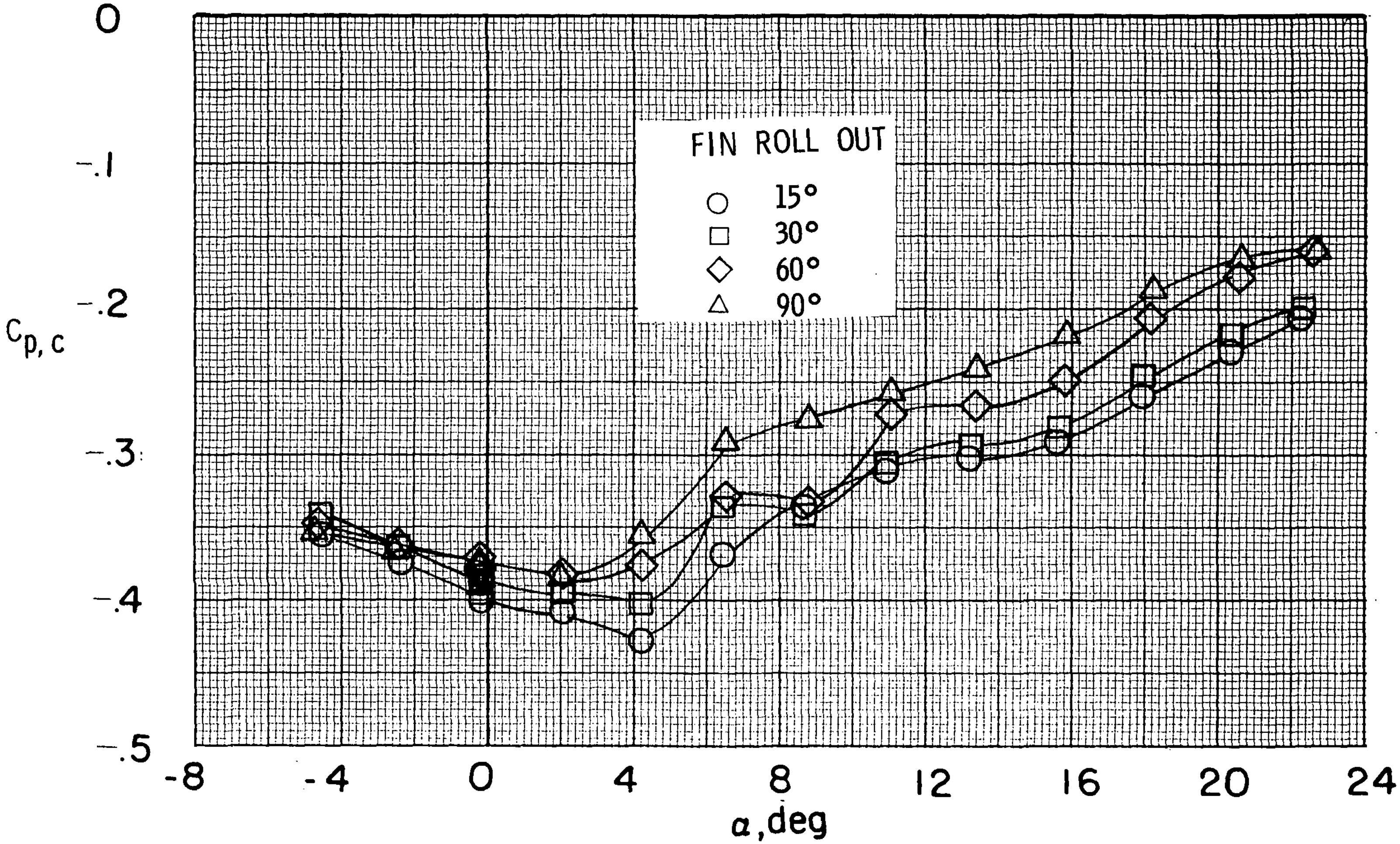

(c) $C_{p,c}$ as a function of α.

Figure 8.- Continued.

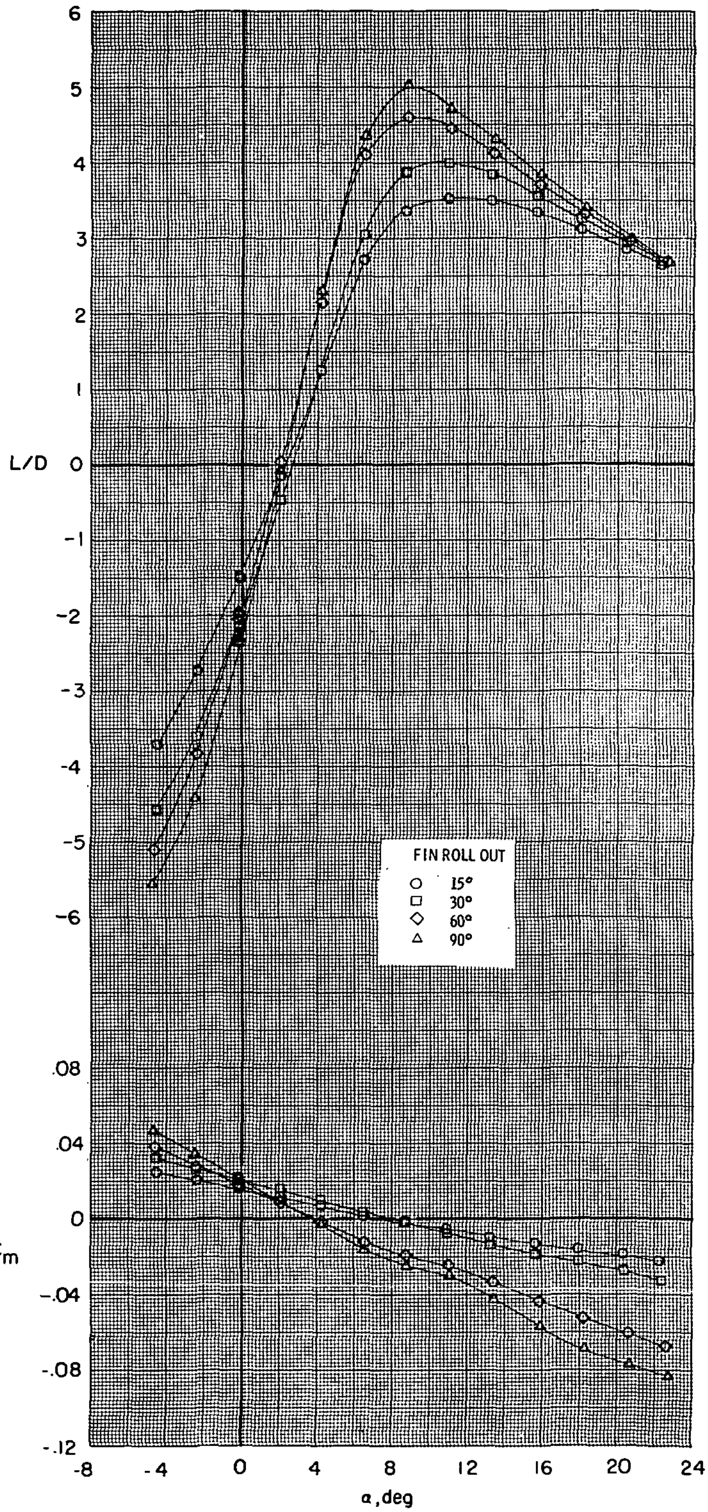

(d) L/D and C_m as a function of α.

Figure 8.- Continued.

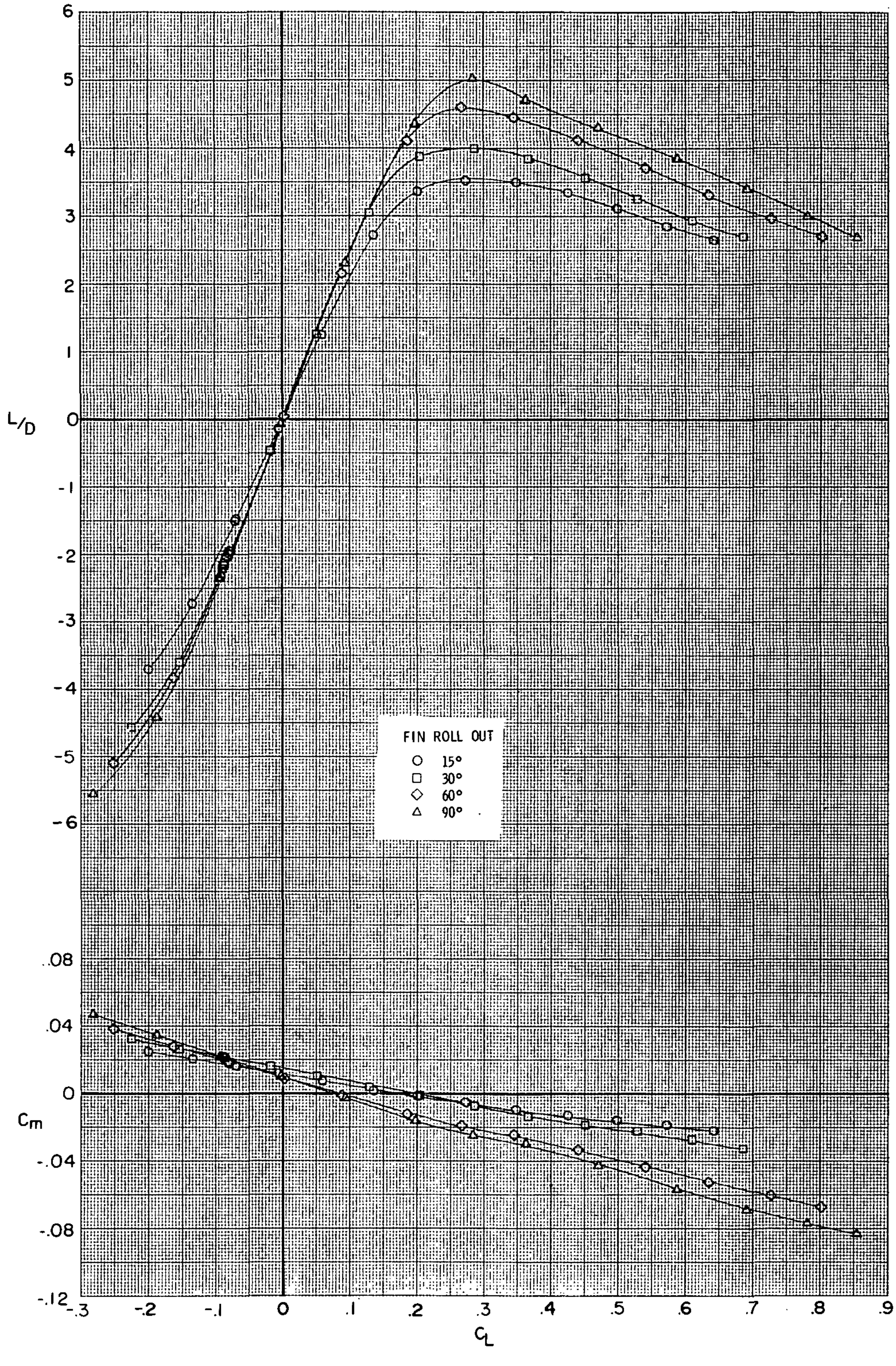

(e) L/D and C_m as a function of C_L.

Figure 8.- Concluded.

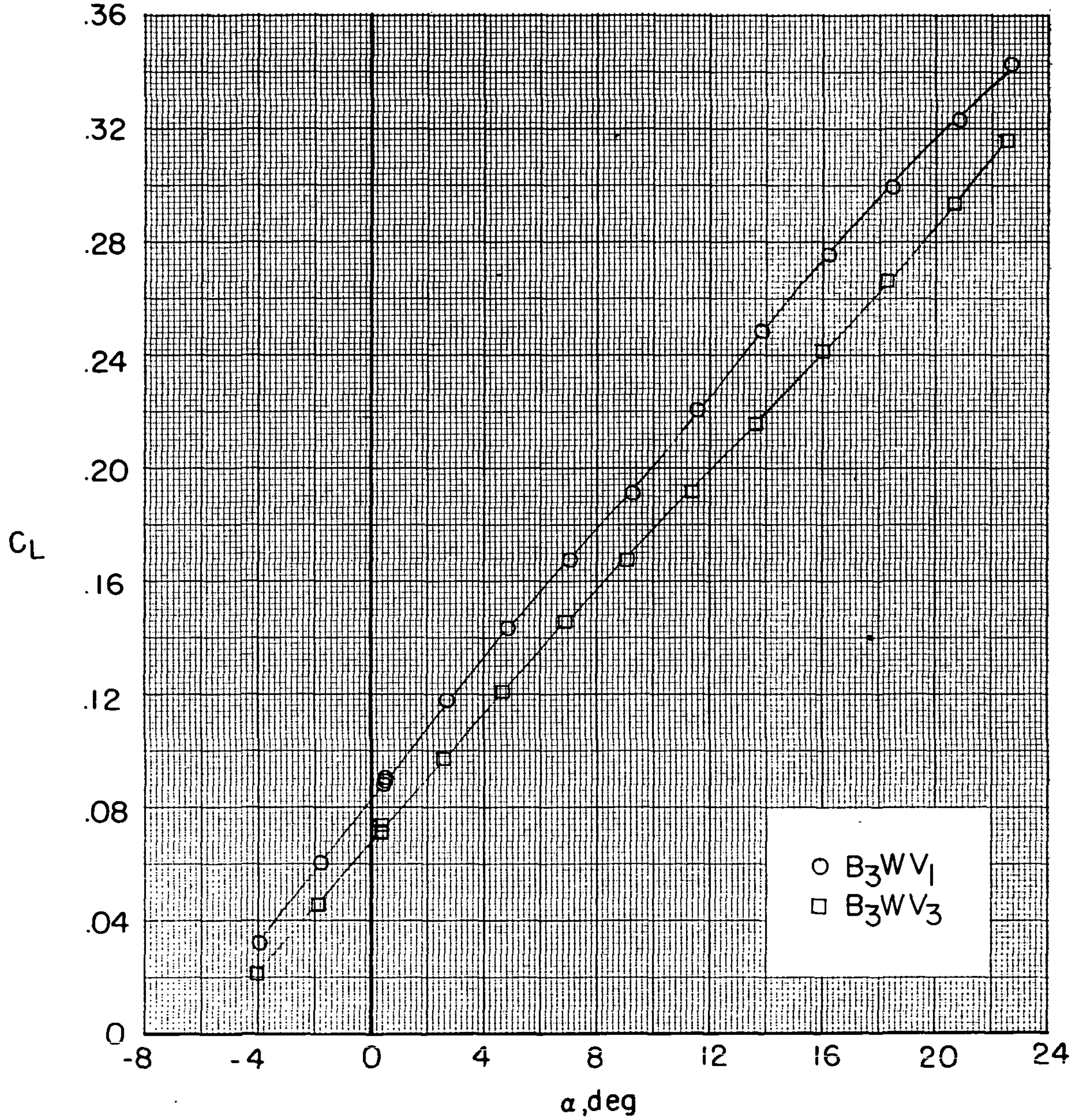

(a) C_L as a function of α.

Figure 9.- Effect of moving tip fins aft on longitudinal characteristics of model. $\delta_e = 0^{\circ}$.

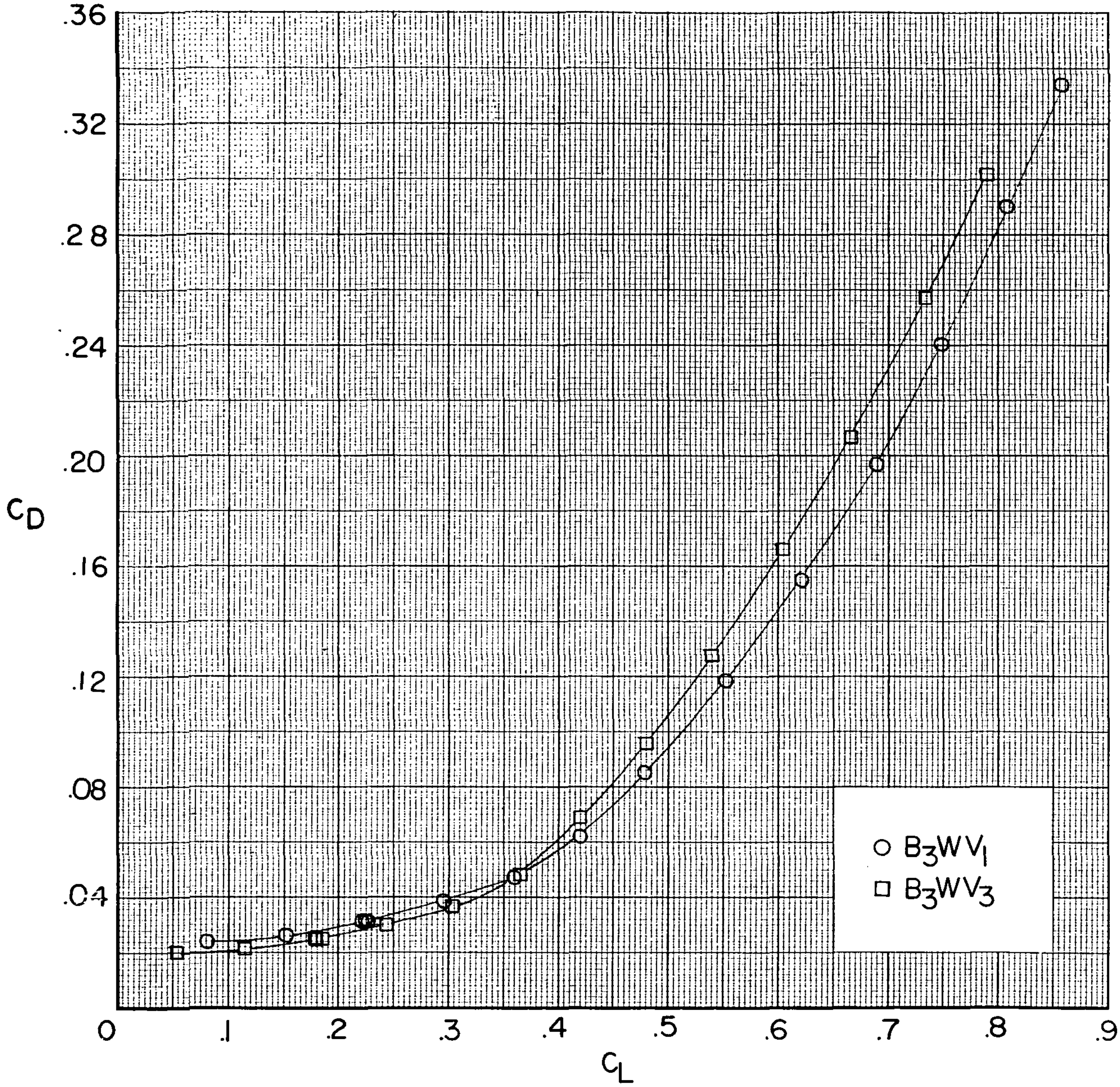

(b) C_D as a function of C_L.

Figure 9.- Continued.

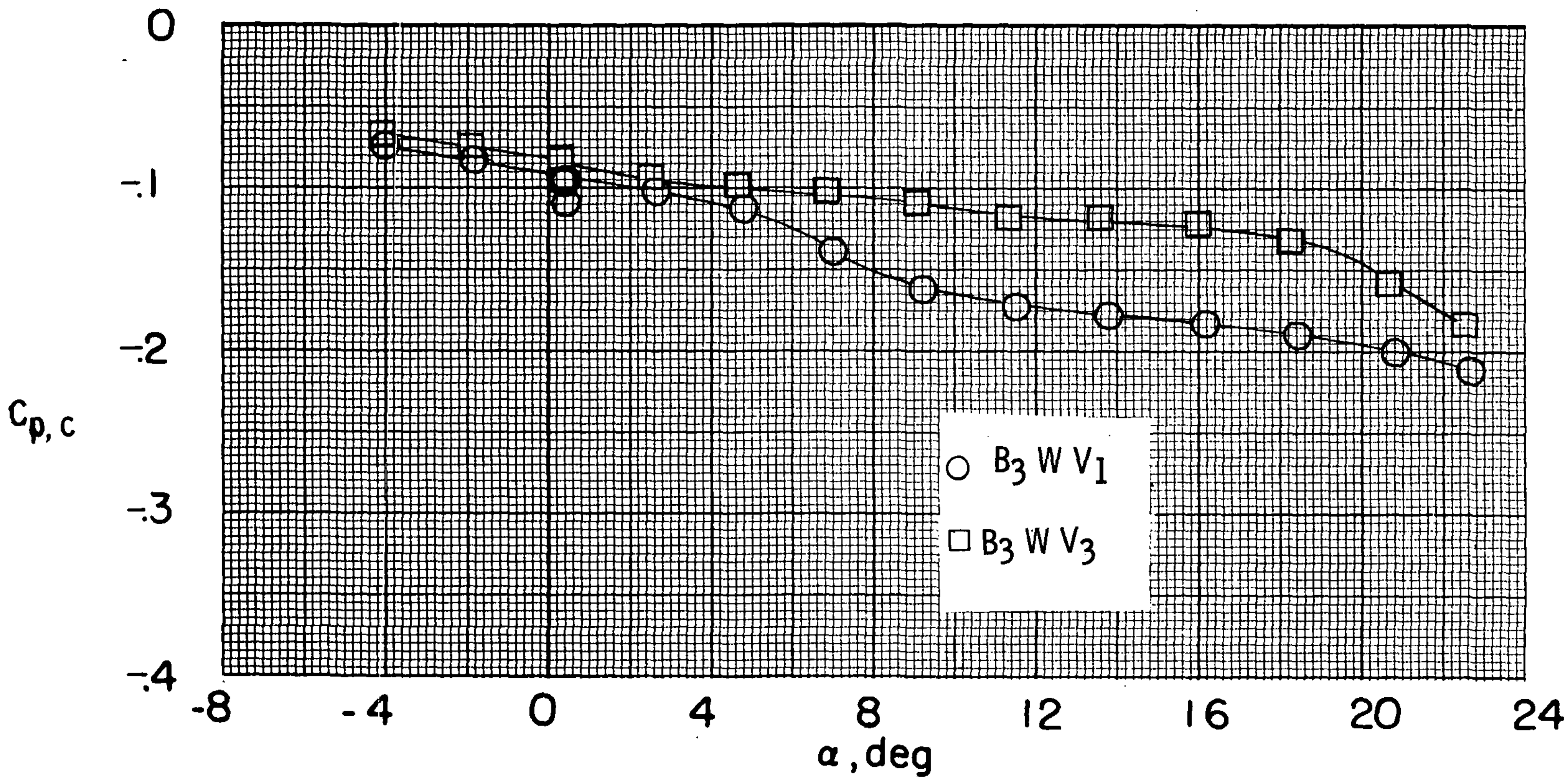

(c) $C_{p,c}$ as a function of α.

Figure 9.- Continued.

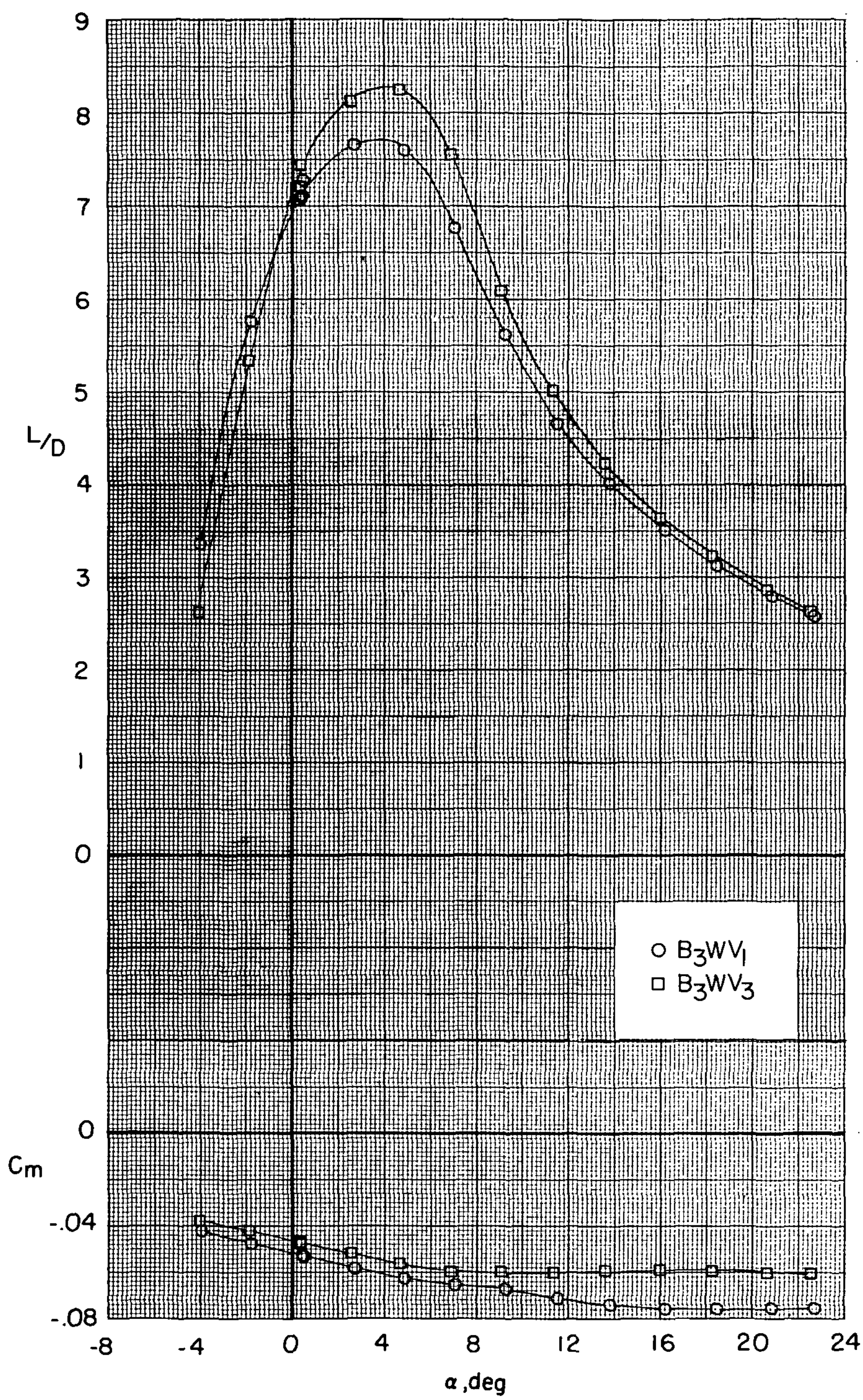

(d) L/D and C_m as a function of α.

Figure 9.- Continued.

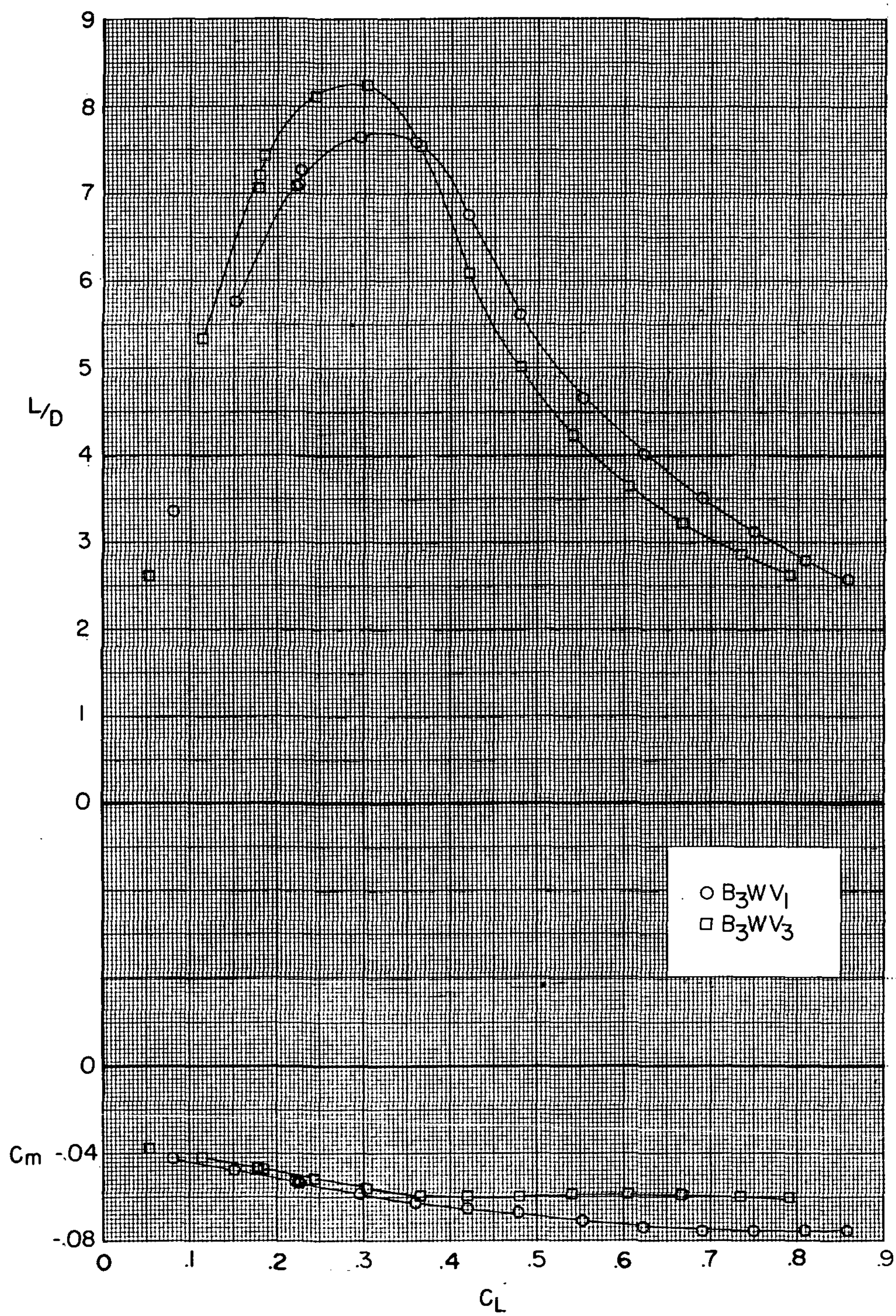

(e) L/D and C_m as a function of C_L.

Figure 9.- Concluded.

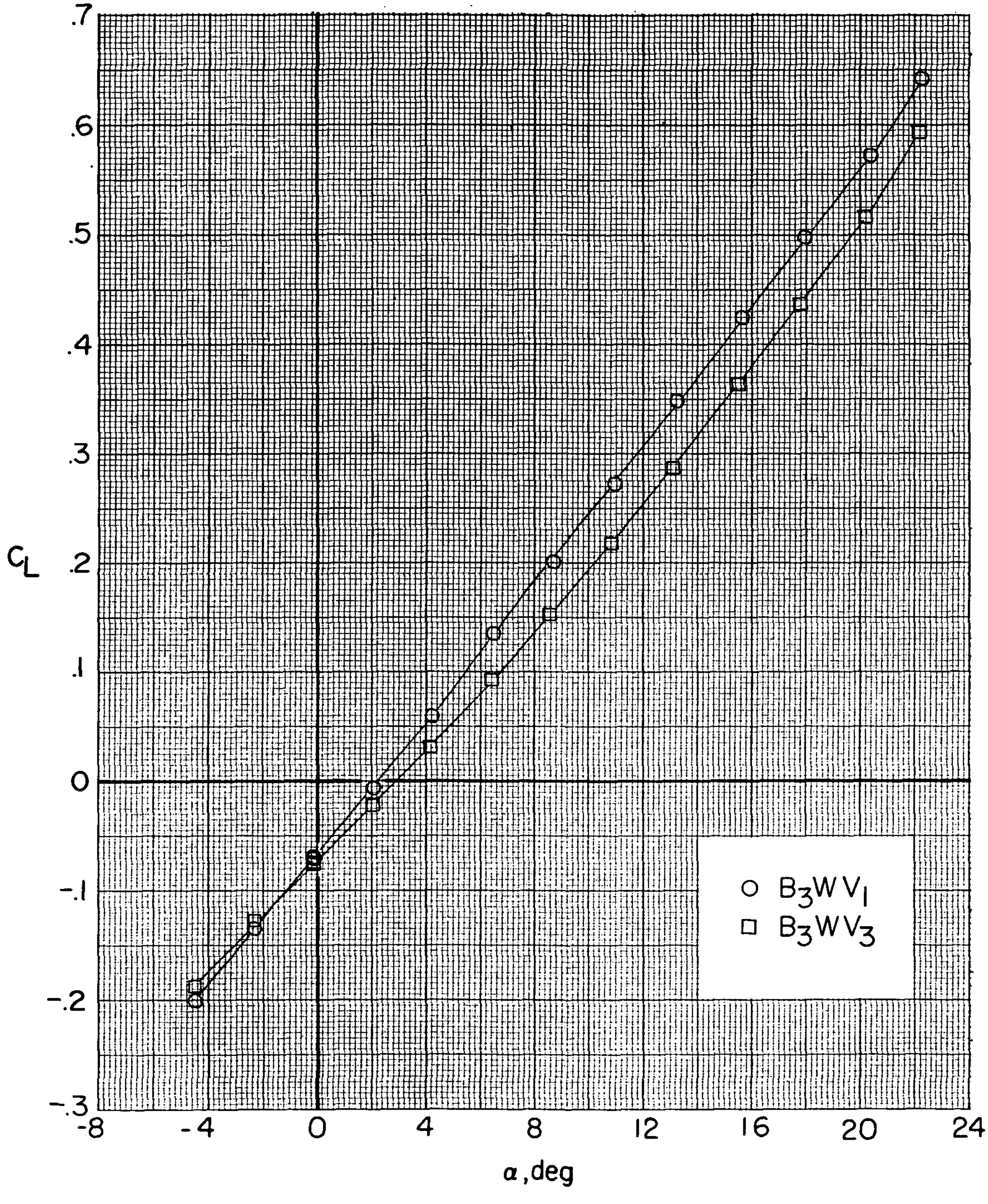

(a) C_L as a function of α.

Figure 10.- Effect of moving tip fins aft on longitudinal characteristics of model. $\delta_e = -30^{\circ}$.

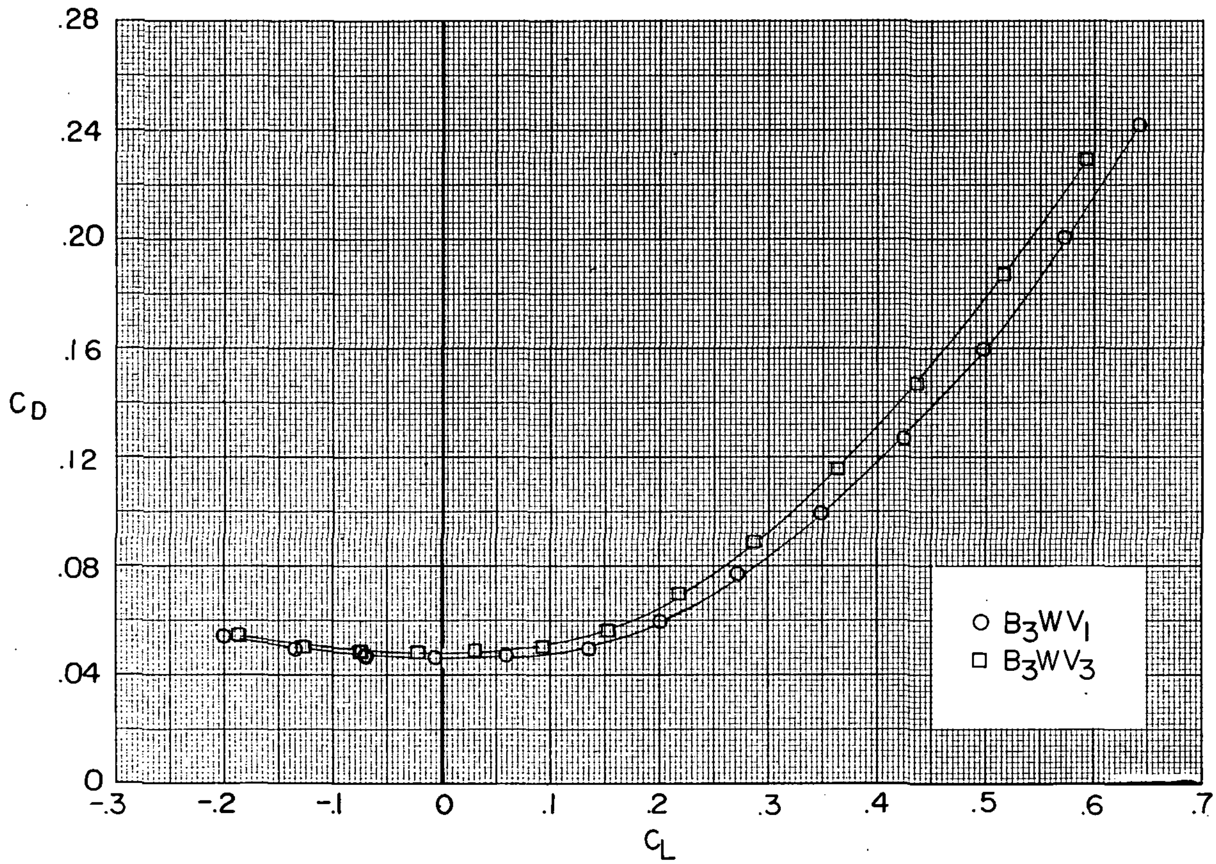

(b) C_D as a function of C_L.

Figure 10.- Continued.

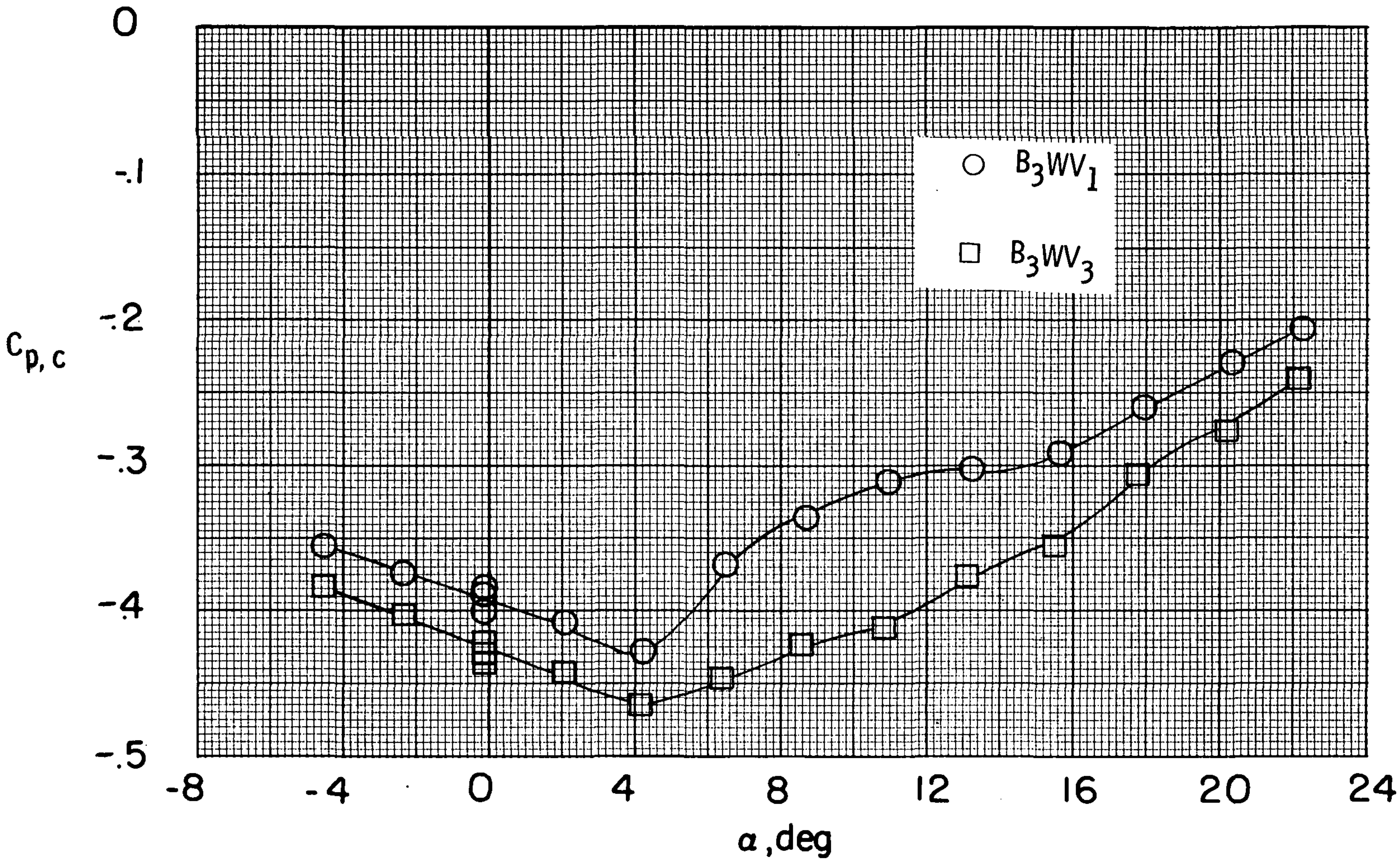

(c) $C_{p,c}$ as a function of α.

Figure 10.- Continued.

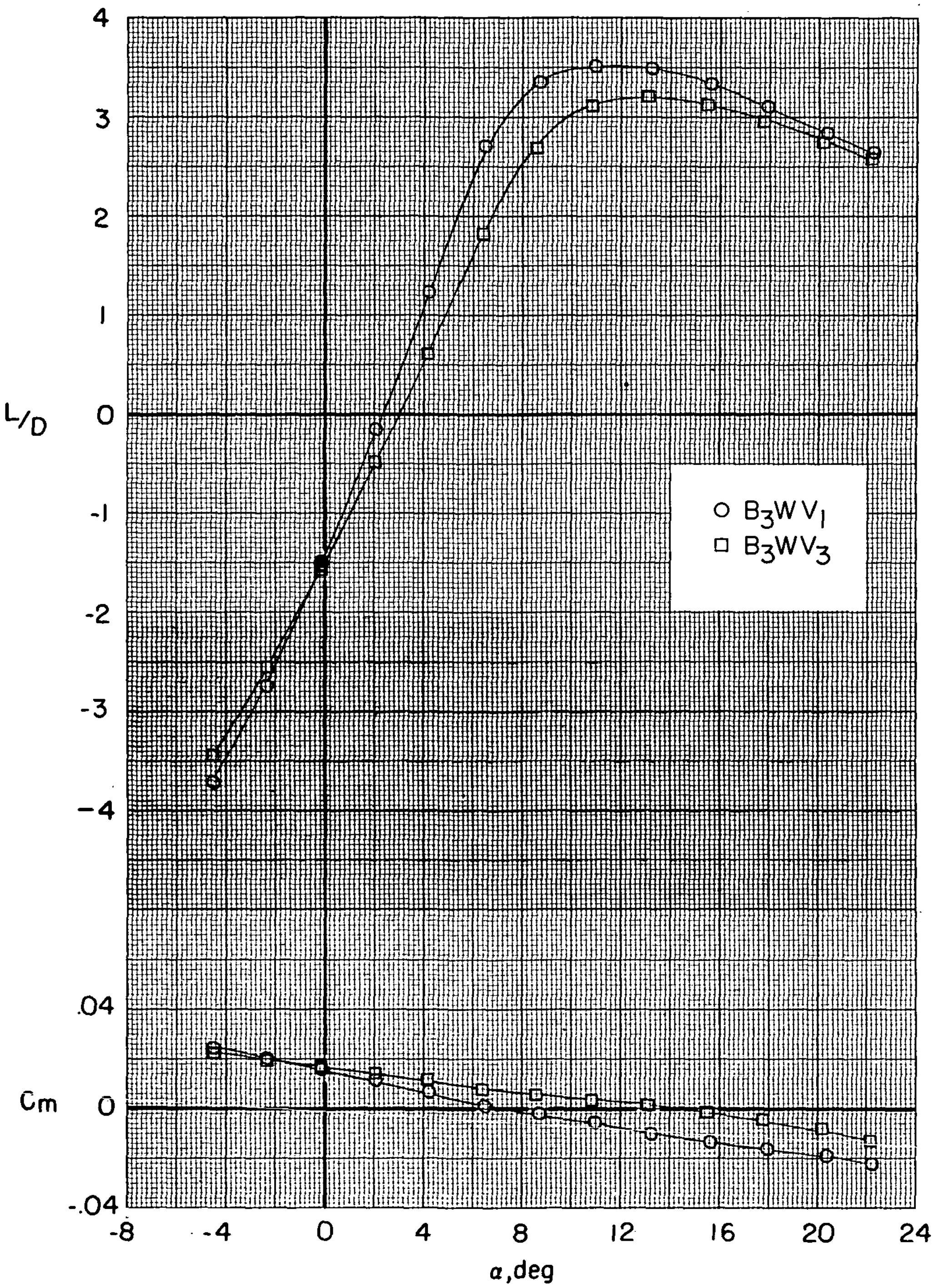

(d) L/D and C_m as a function of α.

Figure 10.- Continued.

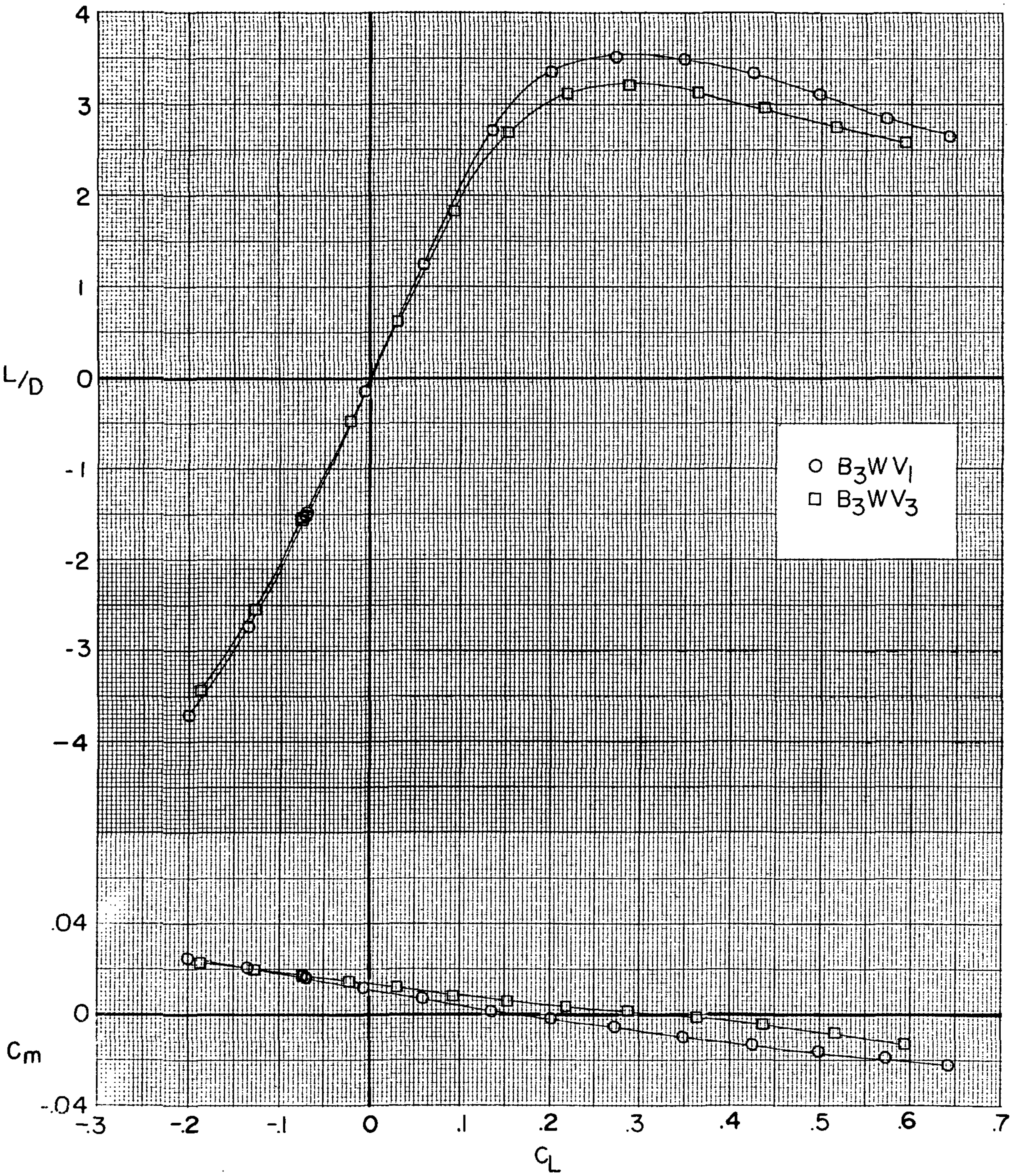

(e) L/D and C_m as a function of C_L.

Figure 10.- Concluded.

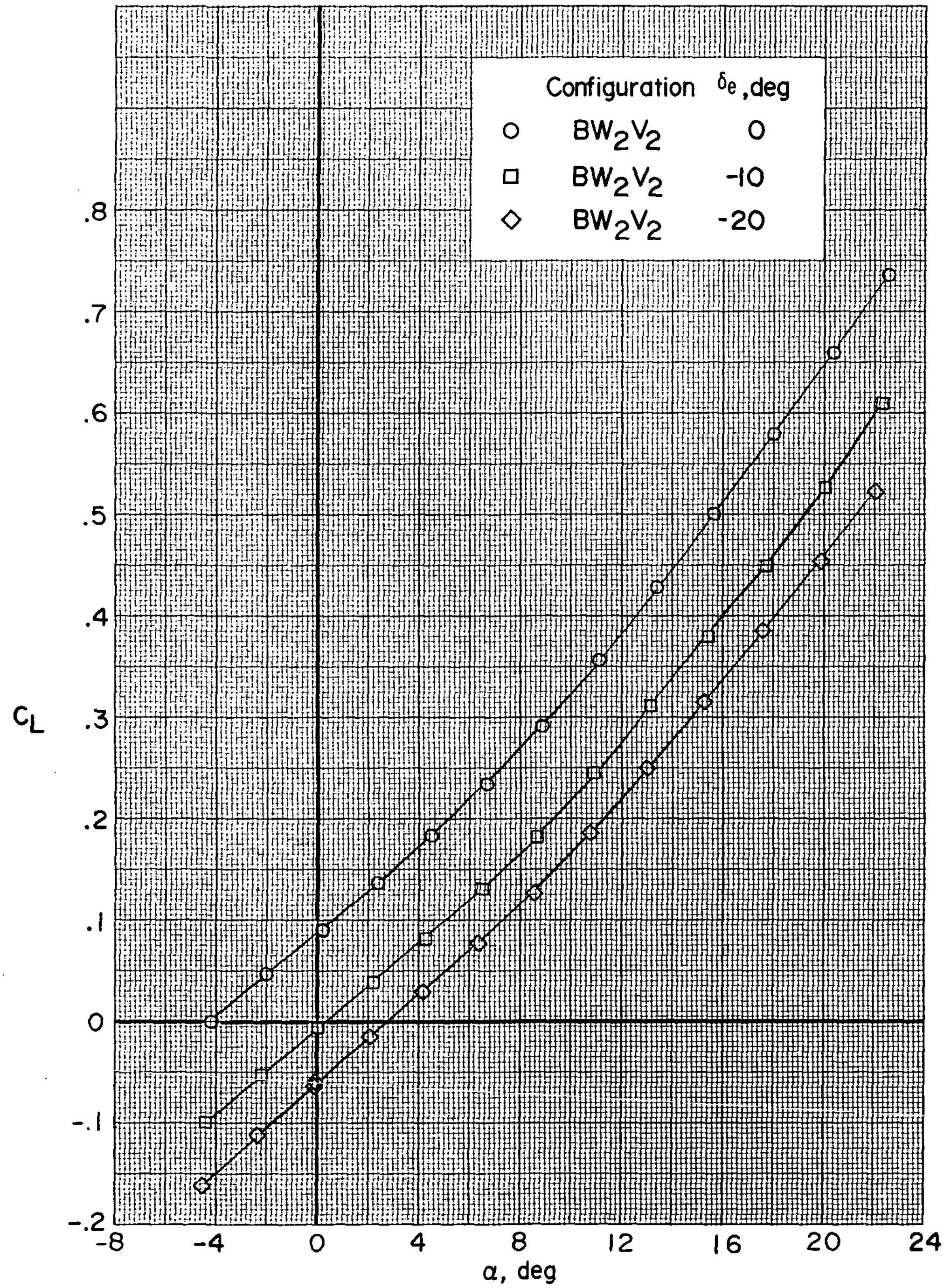

(a) C_L as a function of α.

Figure 11.- Longitudinal control effectiveness of extended-trailing-edge configuration BW_2V_2.

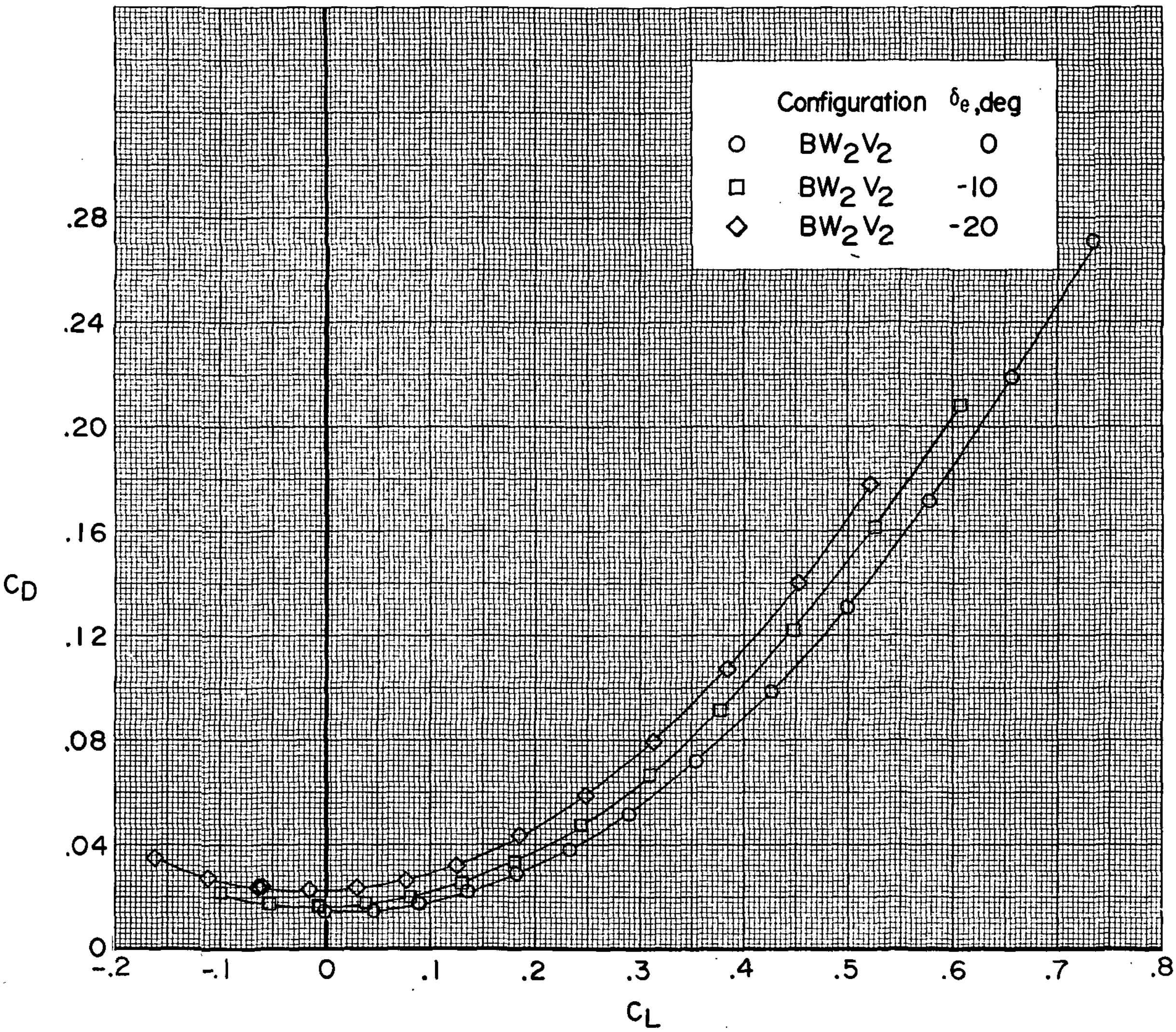

(b) C_D as a function of C_L.

Figure 11.- Continued.

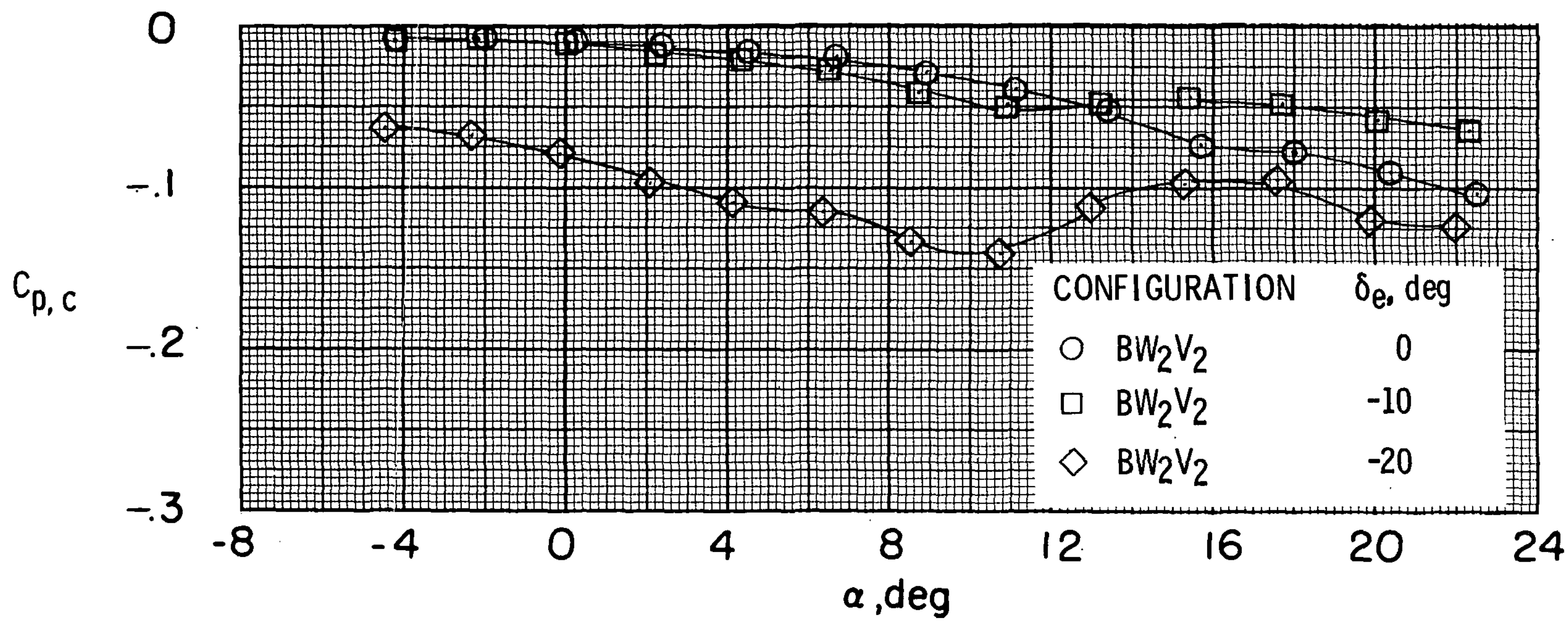

(c) $C_{p,c}$ as a function of α.

Figure 11.- Continued.

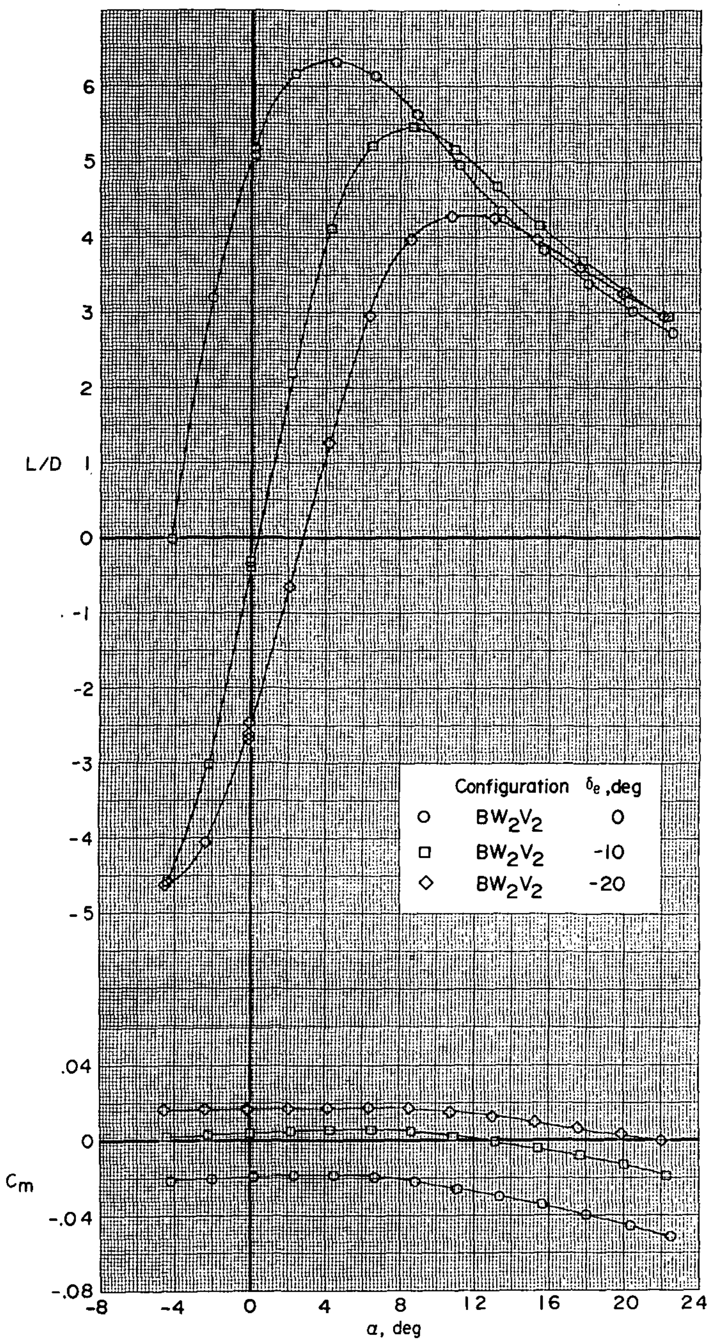

(d) L/D and C_m as a function of α.

Figure 11.- Continued.

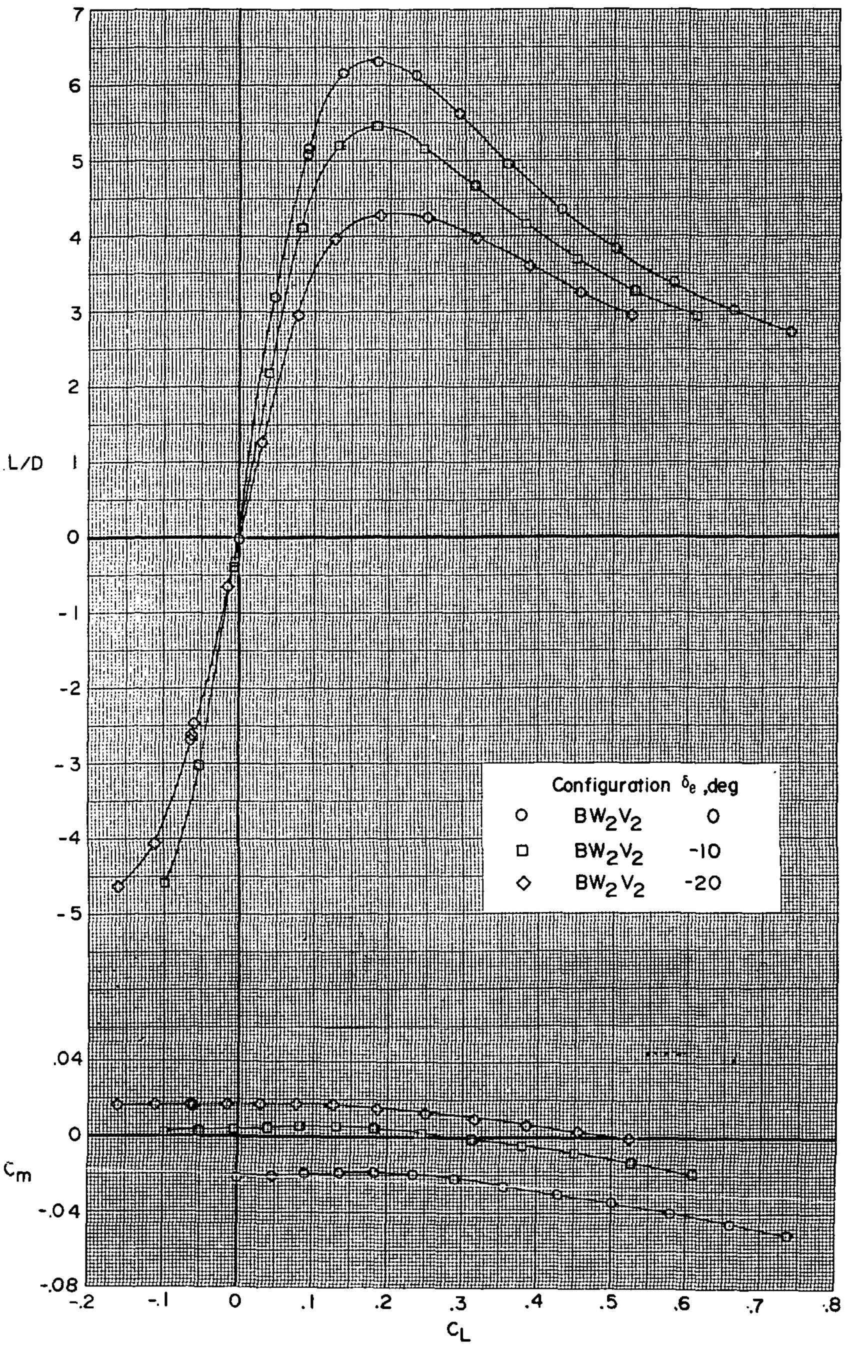

(e) L/D and C_m as a function of C_L.

Figure 11.- Concluded.

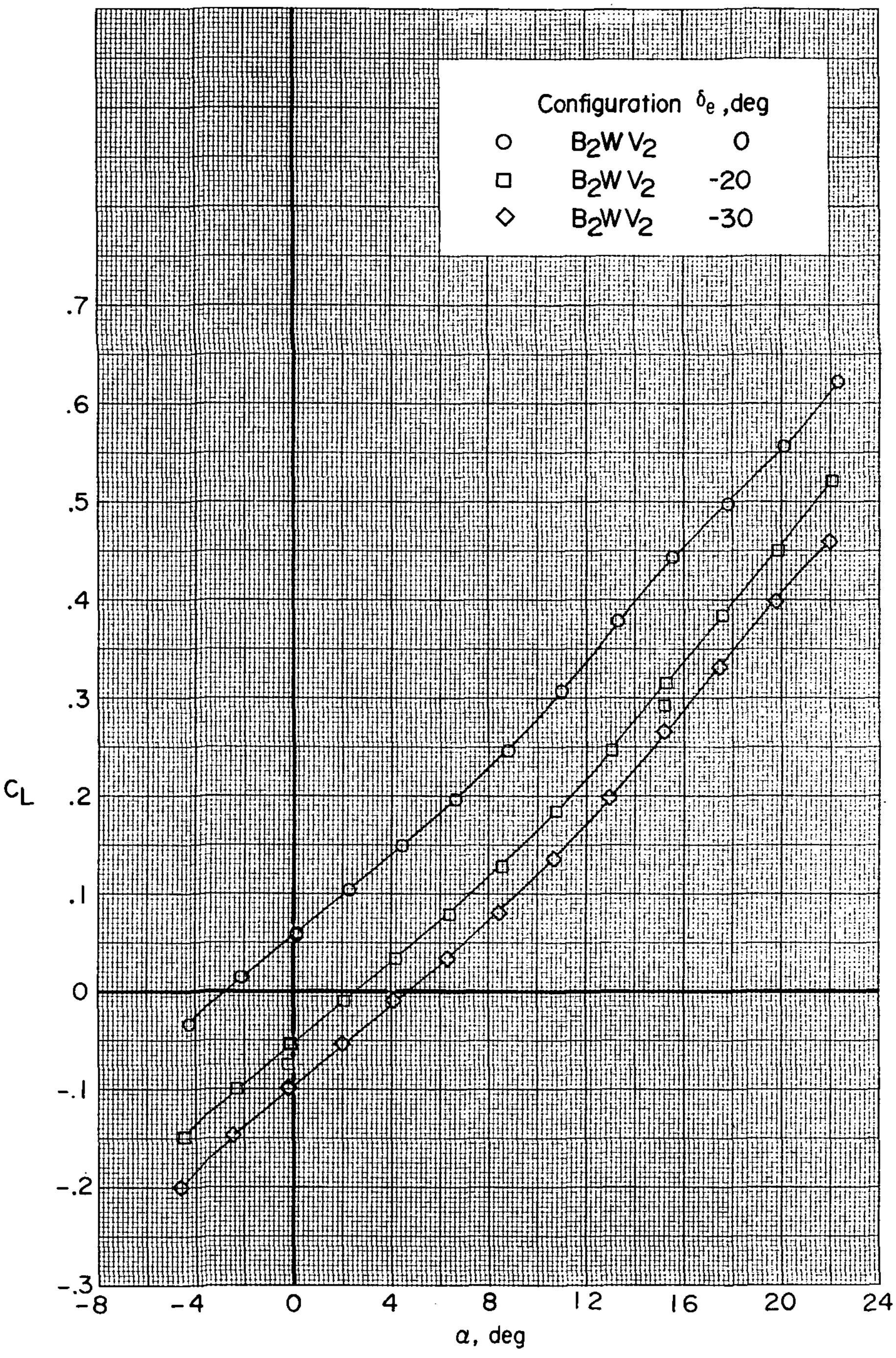

(a) C_L as a function of α.

Figure 12.- Elevon effectiveness of boattailing-removed configuration B_2WV_2.

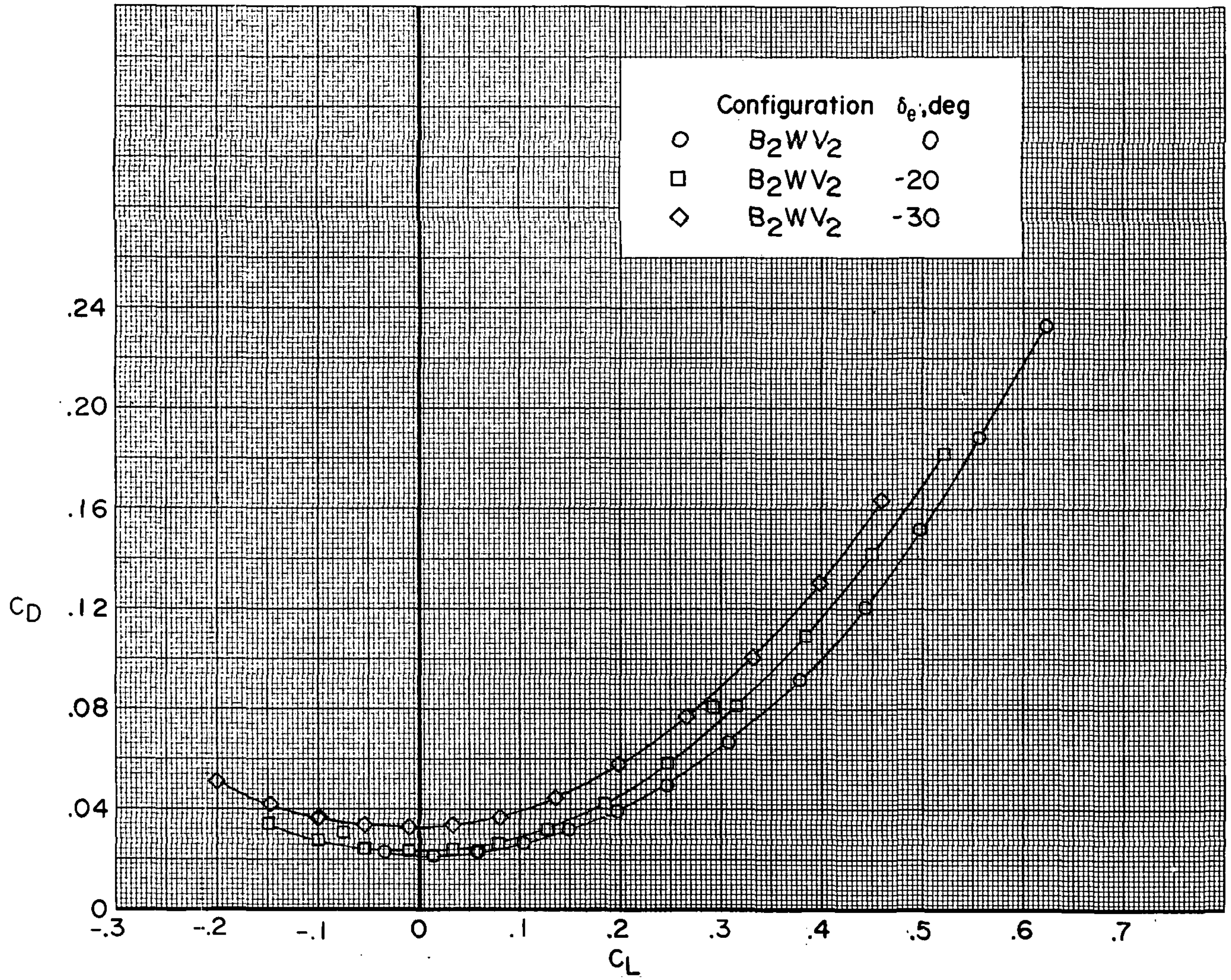

(b) C_D as a function of C_L.

Figure 12.- Continued.

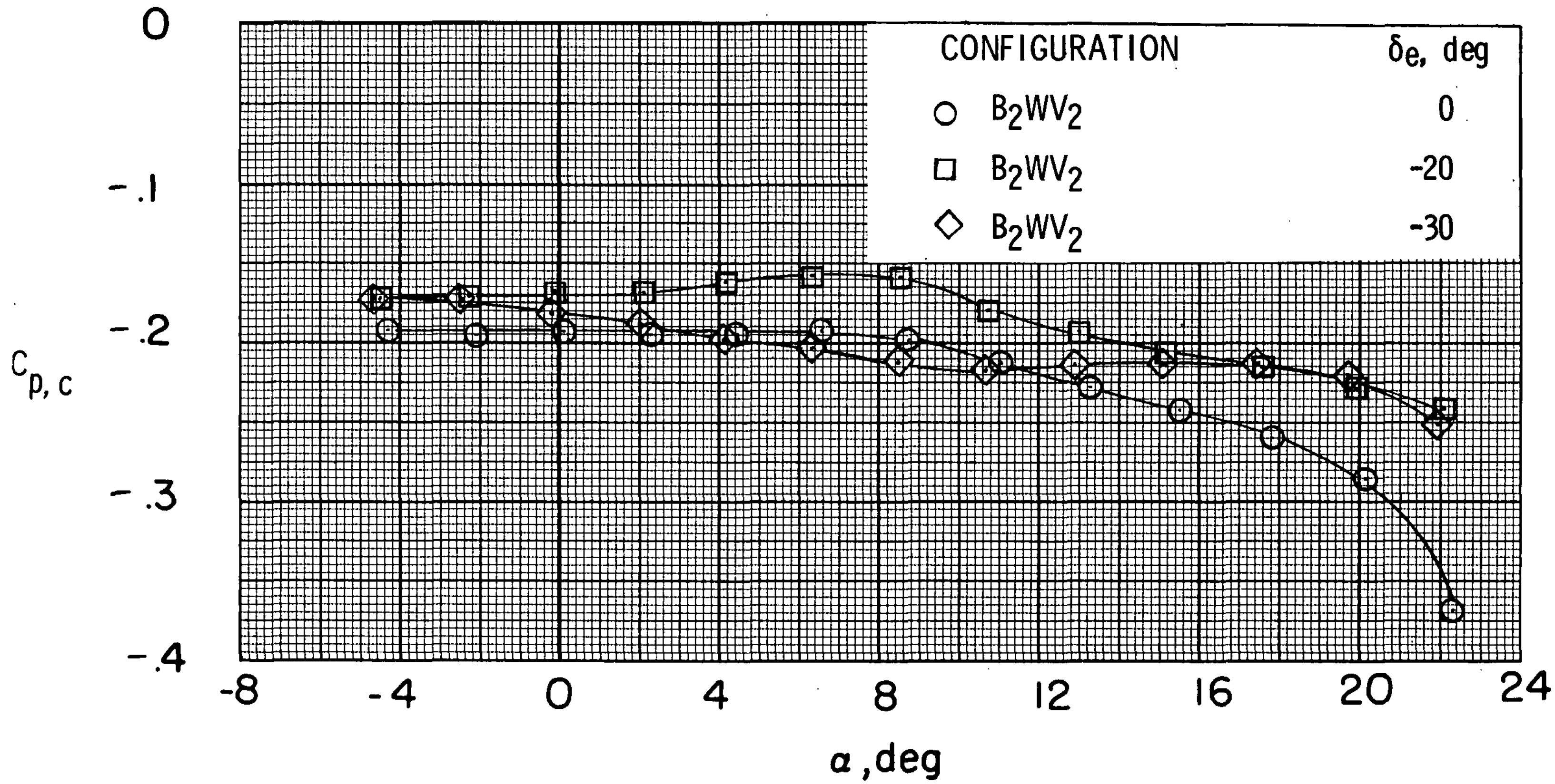

(c) $C_{p,c}$ as a function of α.

Figure 12.- Continued.

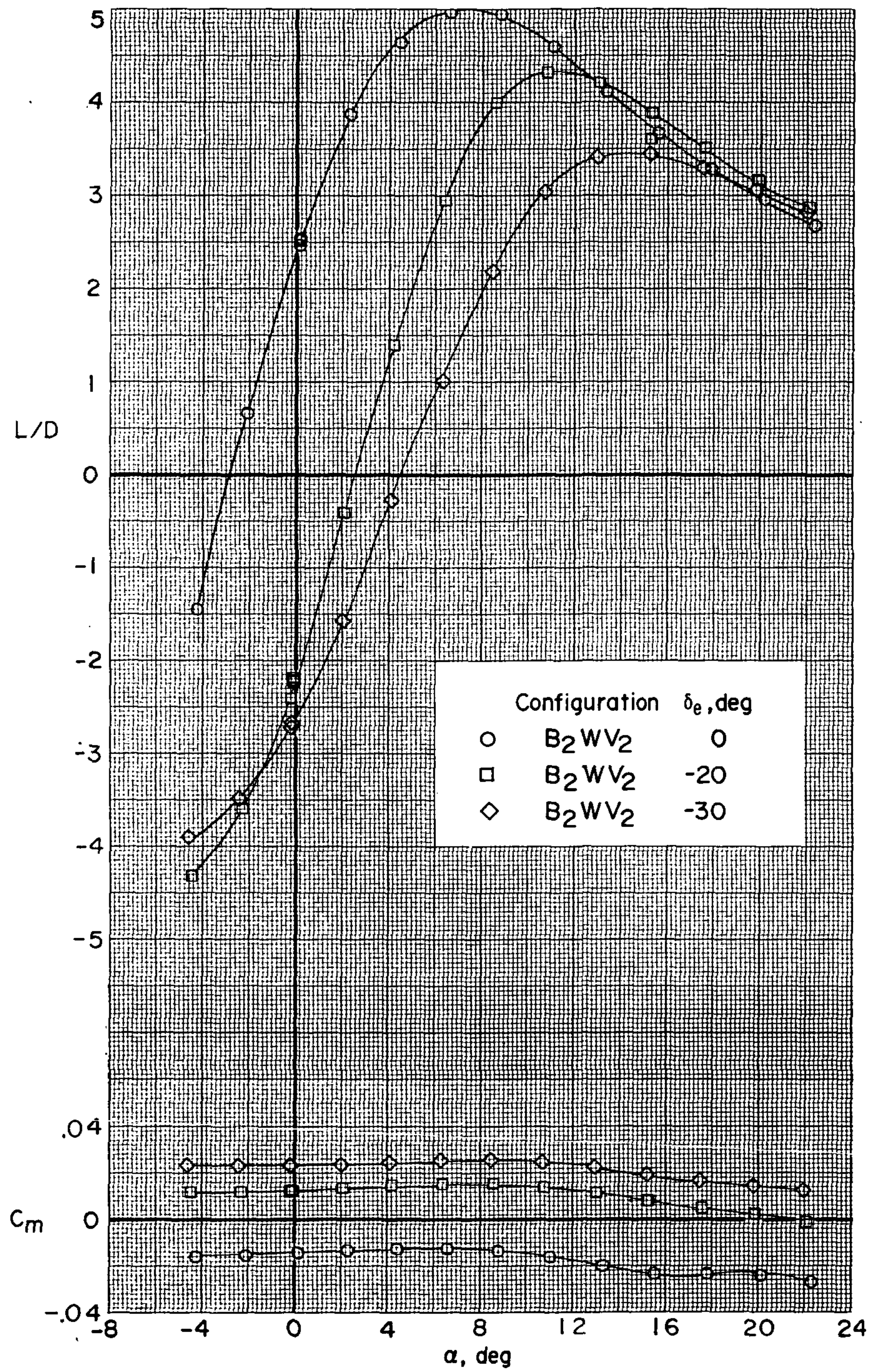

(d) L/D and C_m as a function of α.

Figure 12.- Continued.

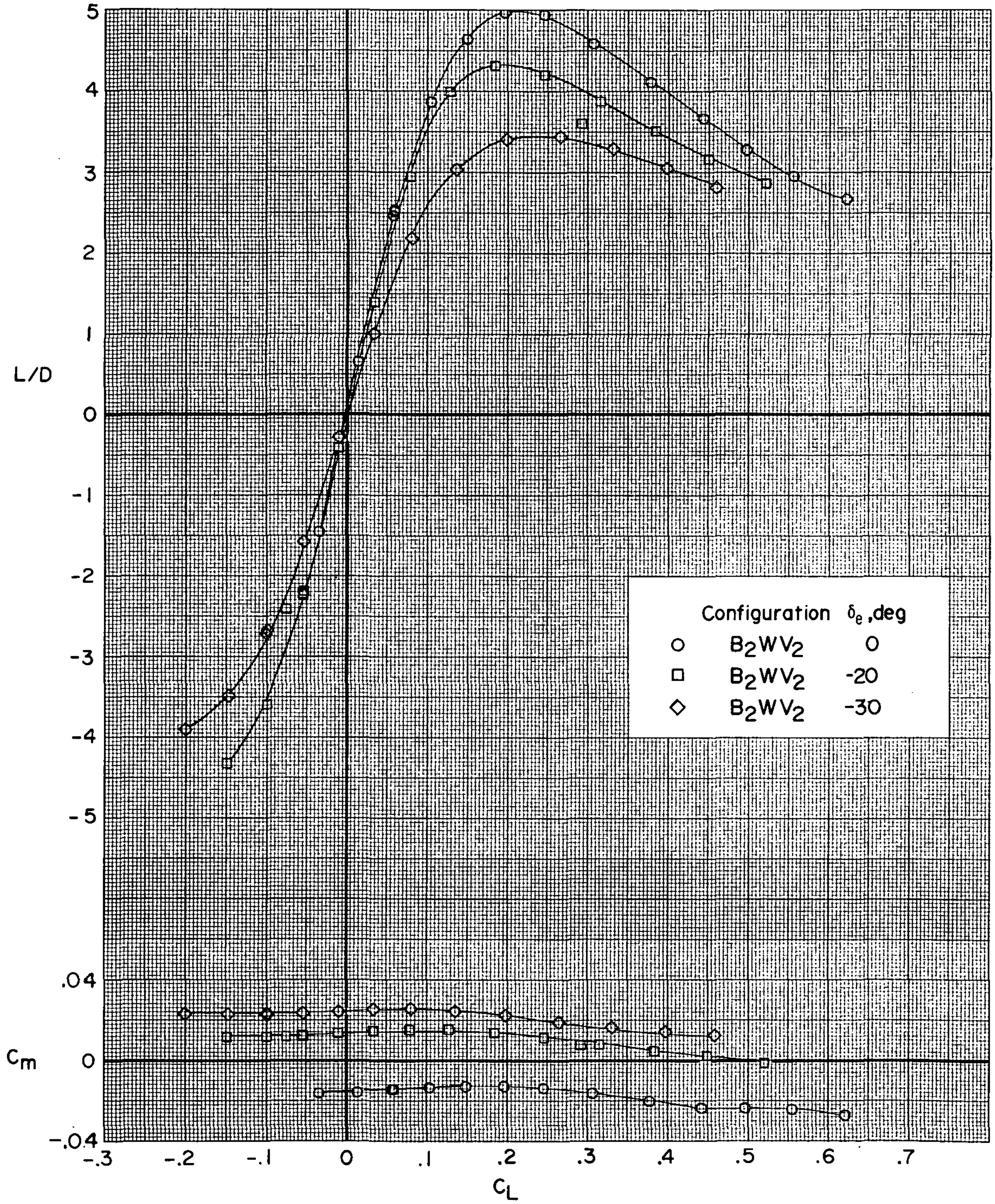

(e) L/D and C_m as a function of C_L.

Figure 12.- Concluded.

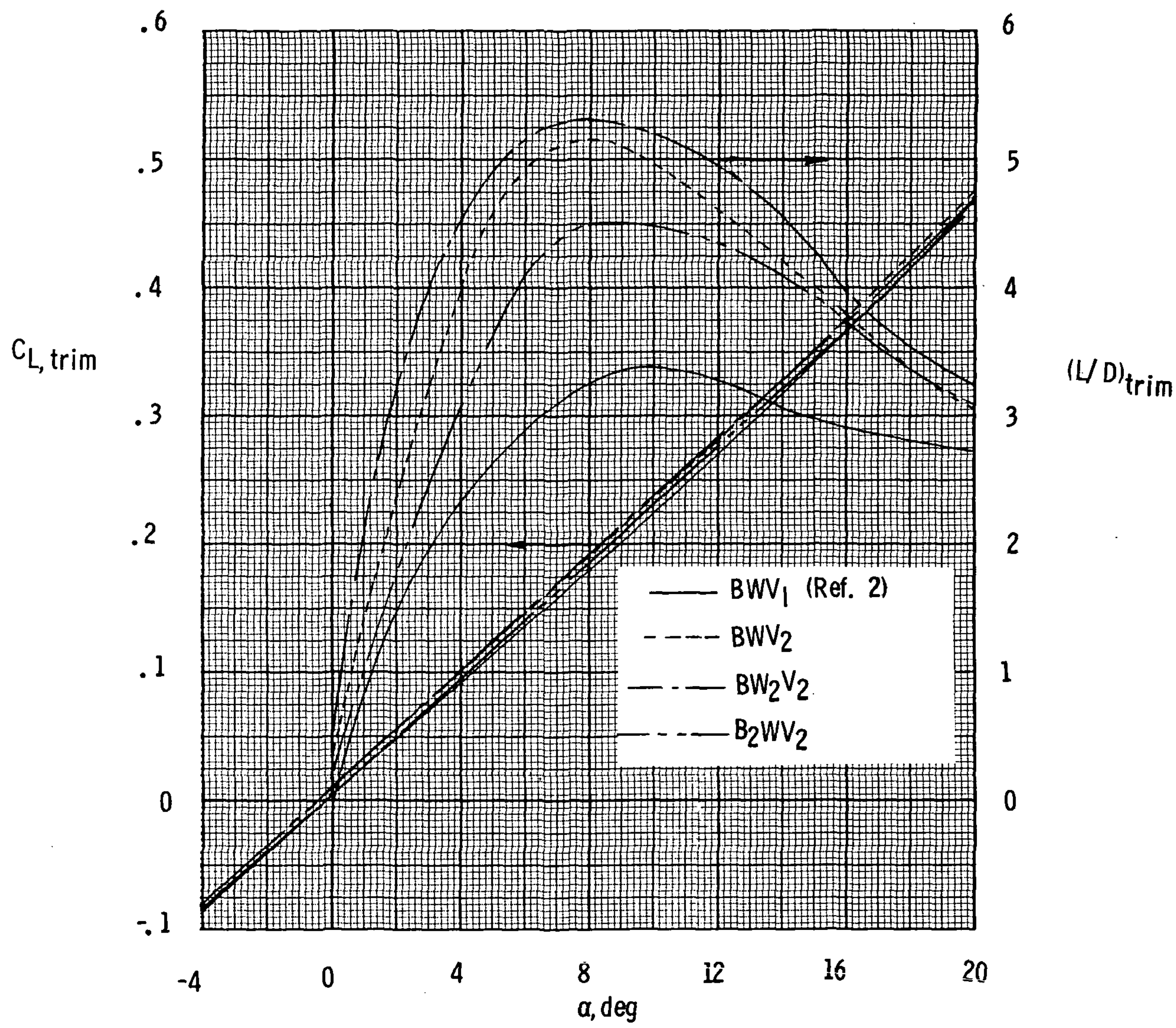

Figure 13.- Longitudinal trim characteristics. Center of gravity at $0.667l$.

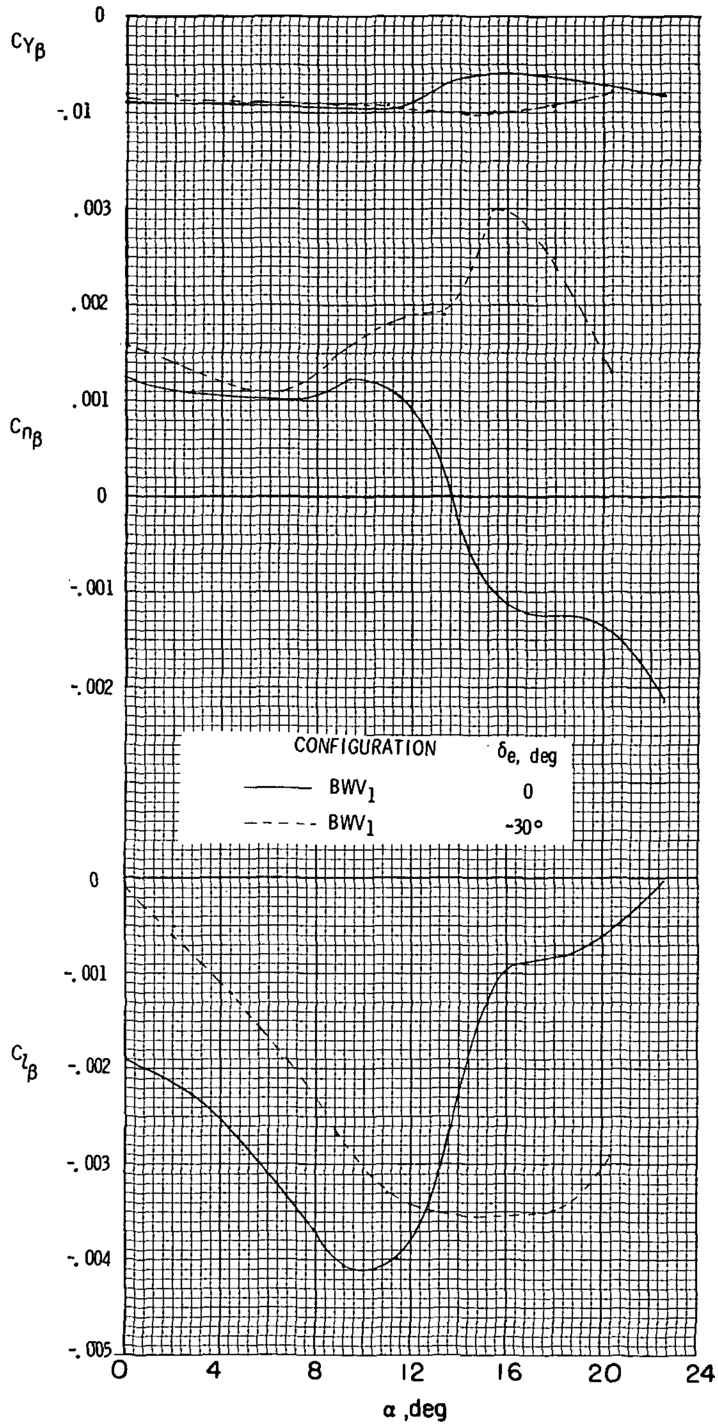

Figure 14.- Effect of elevon deflection on lateral-directional characteristics of configuration BWV_1.

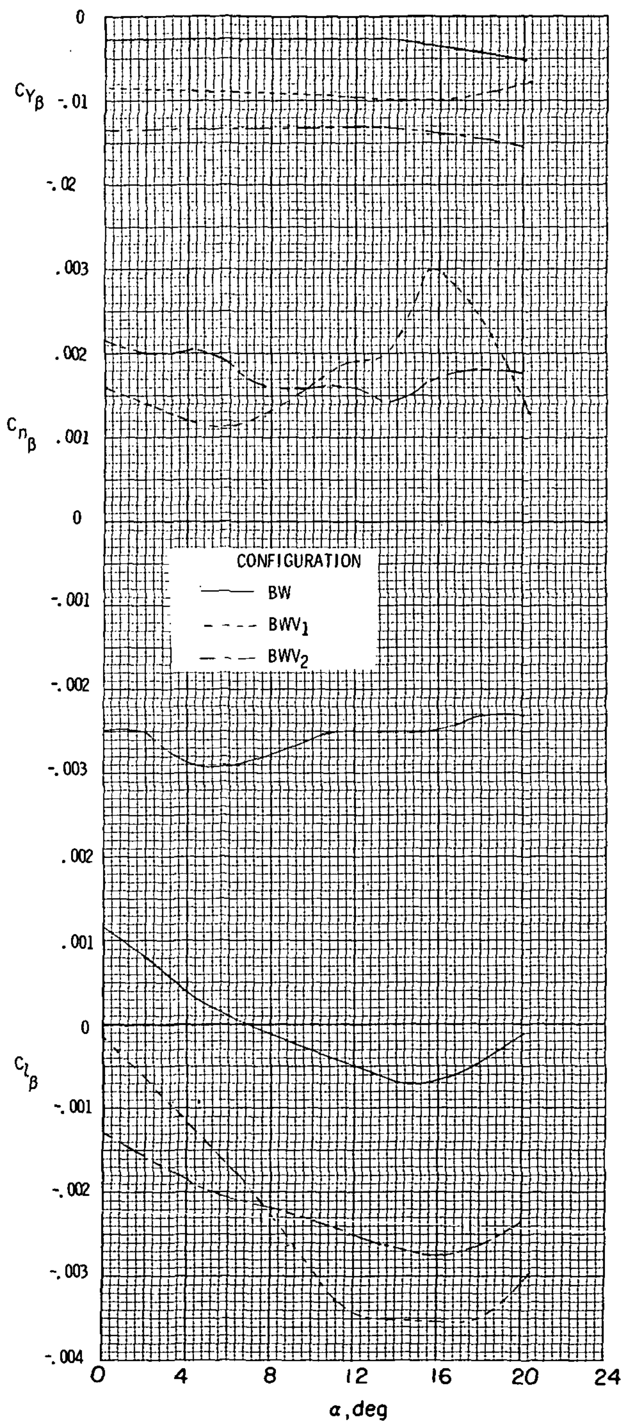

Figure 15.- Effect of vertical-tail configuration on lateral-directional characteristics of model. $\delta_e = -30^{\circ}$.

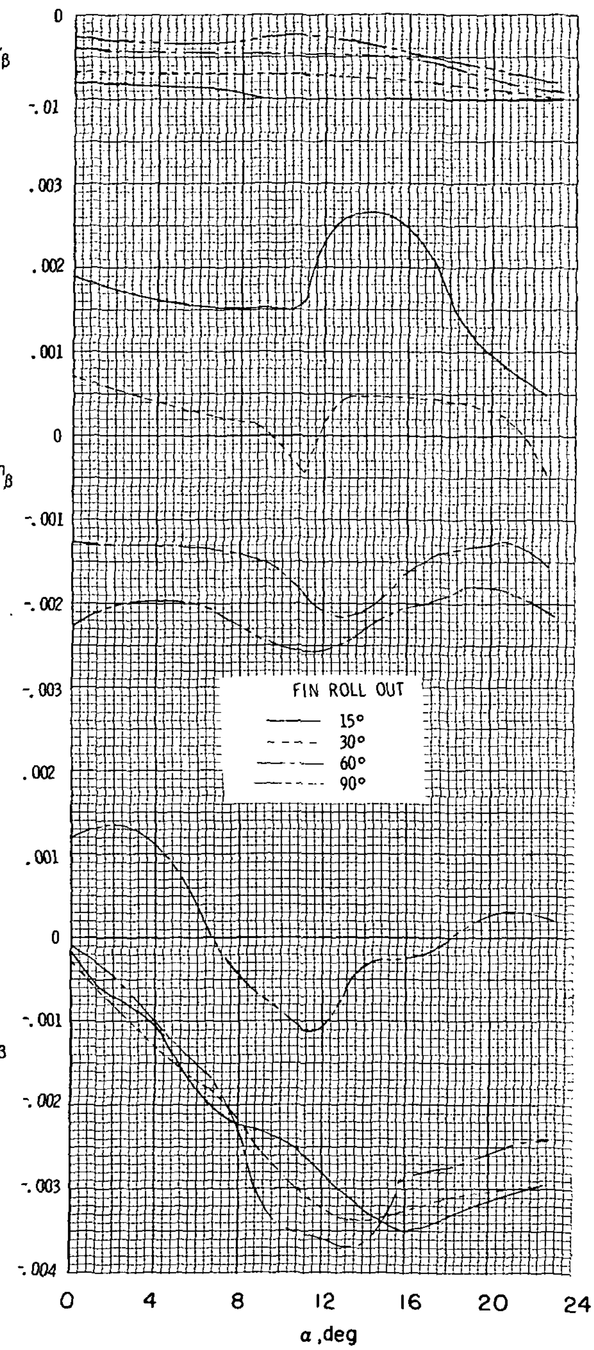

Figure 16.- Effect of fin roll-out angle on lateral-directional characteristics of model. $\delta_e = -30^{\circ}$; configuration B_3WV_1.

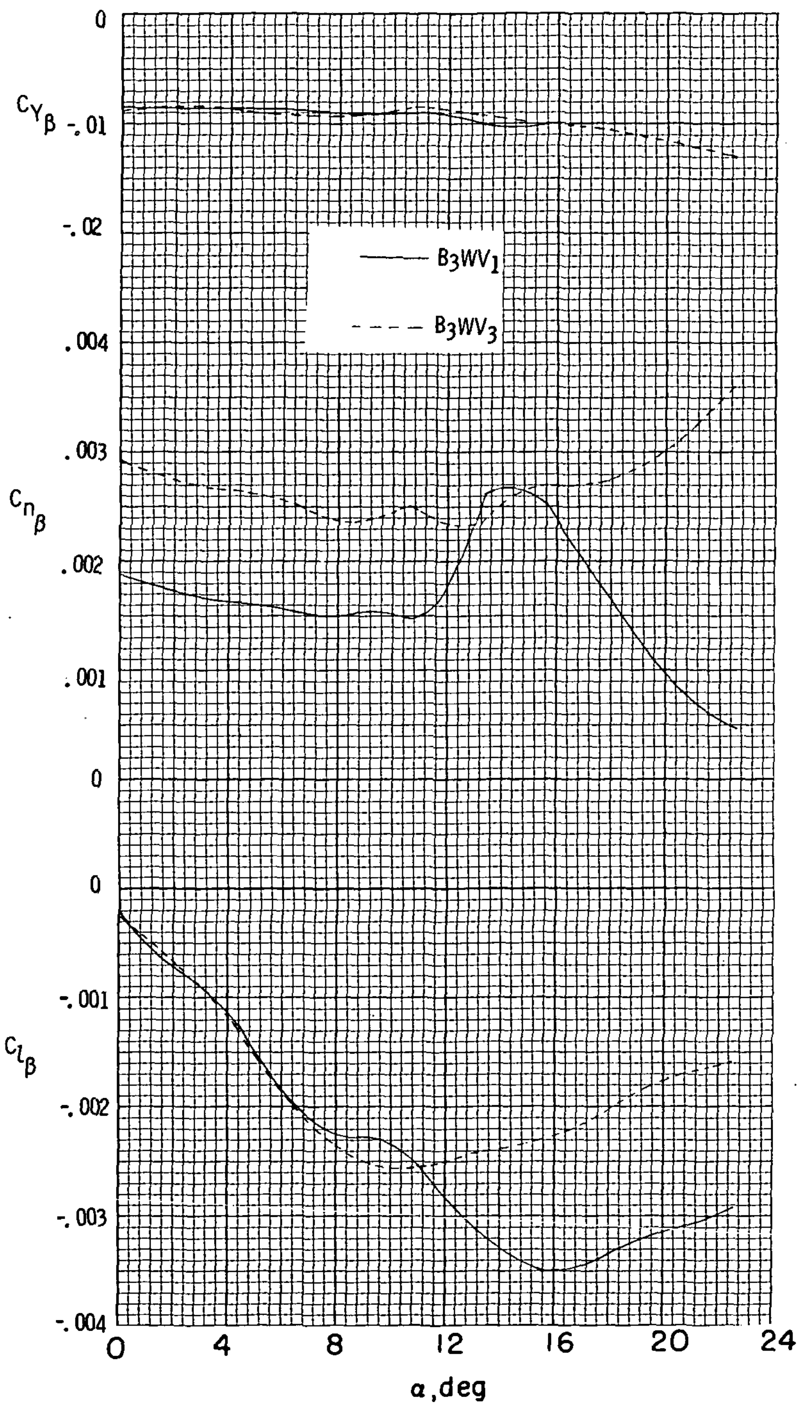

Figure 17.- Effect of moving tip fins aft on lateral-directional characteristics of model. $\delta_e = 0^o$.

"The aeronautical and space activities of the United States shall be conducted so as to contribute . . . to the expansion of human knowledge of phenomena in the atmosphere and space. The Administration shall provide for the widest practicable and appropriate dissemination of information concerning its activities and the results thereof."

—NATIONAL AERONAUTICS AND SPACE ACT OF 1958

NASA SCIENTIFIC AND TECHNICAL PUBLICATIONS

TECHNICAL REPORTS: Scientific and technical information considered important, complete, and a lasting contribution to existing knowledge.

TECHNICAL NOTES: Information less broad in scope but nevertheless of importance as a contribution to existing knowledge.

TECHNICAL MEMORANDUMS: Information receiving limited distribution because of preliminary data, security classification, or other reasons.

CONTRACTOR REPORTS: Scientific and technical information generated under a NASA contract or grant and considered an important contribution to existing knowledge.

TECHNICAL TRANSLATIONS: Information published in a foreign language considered to merit NASA distribution in English.

SPECIAL PUBLICATIONS: Information derived from or of value to NASA activities. Publications include conference proceedings, monographs, data compilations, handbooks, sourcebooks, and special bibliographies.

TECHNOLOGY UTILIZATION PUBLICATIONS: Information on technology used by NASA that may be of particular interest in commercial and other non-aerospace applications. Publications include Tech Briefs, Technology Utilization Reports and Technology Surveys.

Details on the availability of these publications may be obtained from:

SCIENTIFIC AND TECHNICAL INFORMATION OFFICE

NATIONAL AERONAUTICS AND SPACE ADMINISTRATION
Washington, D.C. 20546